

การพัฒนา Mg-PSZ ดันทุนต่ำให้มีโครงสร้างระดับนาโนและมีความแข็งแรงเชิงกลสูง



นางสาว ปวีณา ตันงาม

สถาบันวิทยบริการ

จุฬาลงกรณ์มหาวิทยาลัย

วิทยานิพนธ์นี้เป็นส่วนหนึ่งของการศึกษาตามหลักสูตรปริญญาวิทยาศาสตรมหาบัณฑิต

สาขาวิชาเทคโนโลยีเซรามิก ภาควิชาวัสดุศาสตร์


คณะวิทยาศาสตร์ จุฬาลงกรณ์มหาวิทยาลัย

ปีการศึกษา 2547

ISBN 974-17-6401-4

ลิขสิทธิ์ของจุฬาลงกรณ์มหาวิทยาลัย

DEVELOPMENT OF LOW COST Mg-PSZ WITH NANOSTRUCTURE
AND HIGH MECHANICAL STRENGTH



Miss Pawena Thanngam

สถาบันวิทยบริการ
จุฬาลงกรณ์มหาวิทยาลัย

A Thesis Submitted in Partial Fulfillment of the Requirements
for the Degree of Master of Science in Ceramic Technology

Department of Materials Science

Faculty of Science

Chulalongkorn University

Academic Year 2004

ISBN 974-17-6401-4

ปีถัดมา : การพัฒนา Mg-PSZ ต้นทุนต่ำให้มีโครงสร้างระดับนาโนและมีความแข็งแรงเชิงกลสูง. (DEVELOPMENT OF LOW COST Mg-PSZ WITH NANOSTRUCTURE AND HIGH MECHANICAL STRENGTH) อ. ที่ปรึกษา : ศ. ดร. ชิกตะกะ วาดะ, อ.ที่ปรึกษาร่วม : รศ.ดร สุพัตรา จินวัฒน์, 52 หน้า. ISBN : 974-17-6401-4

Mg-PSZ เป็นวัสดุที่นิยมนำมาใช้ในงานในเชิงวิศวกรรม เนื่องจากเป็นวัสดุเซรามิกที่เมื่อผ่านการเผาซินเทอร์แล้วจะมี fracture toughness สูง การเติมแมกนีเซียมลงไปในเซอร์โคเนียทำให้เกิด metastable tetragonal phase กระจายตัวอยู่ในคิวบิกเมตริกซ์ของเซอร์โคเนีย ทัวไปนิยมเติมลงไปประมาณ 8-10 โมลเปอร์เซ็นต์ เชื่อกันว่า toughness ที่สูงของ Mg-PSZ เป็นผลมาจาก tetragonal zirconia phase ที่กระจายอย่างสม่ำเสมอในคิวบิกเซอร์โคเนียเกรน นอกจากนี้สมบัติเชิงกลและสมบัติทางความร้อนของ Mg-PSZ ยังสามารถปรับปรุงได้โดยการควบคุมโครงสร้างจุลภาคโดยกระบวนการอิทธิพริทเมนต์

งานวิจัยนี้มีจุดประสงค์ที่จะศึกษาถึงการเปลี่ยนแปลงและสมบัติเชิงกลของ Mg-PSZ ที่เติมแมกนีเซียมออกไซด์ 8.1 โมลเปอร์เซ็นต์ โดยนำชิ้นทดลองที่ผ่านการขึ้นรูปแล้ว มาทำการเผาซินเทอร์ในช่วงอุณหภูมิ 1500 ถึง 1700 องศาเซลเซียส เป็นเวลา 2 ชั่วโมง จากนั้นนำไปทำอิทธิพริทเมนต์ที่อุณหภูมิ 1400 องศาเซลเซียส ในช่วงเวลา 0.5 ถึง 10 ชั่วโมง ในบรรยากาศปกติ เพื่อหลีกเลี่ยงการเกิด eutectoid decomposition ที่อุณหภูมิต่ำ

ชิ้นงานที่ผ่านการเผาที่อุณหภูมิ 1700 องศาเซลเซียส มีความหนาแน่น 5.78 กรัมต่อลูกบาศก์เซนติเมตร ซึ่งเป็นค่าที่ใกล้เคียงกับค่าความหนาแน่นทางทฤษฎี เมื่อเพิ่มอุณหภูมิในการเผาซินเทอร์ ความแข็งแรงและความทนแรงดัดโค้งของชิ้นงานลดลง แต่ fracture toughness เพิ่มขึ้น หลังจากการทำอิทธิพริทเมนต์ความแข็งแรงและความทนแรงดัดโค้งจะลดลงมาก ชิ้นงานที่ถูกเผาที่อุณหภูมิต่ำกว่าจะเกิดการเปลี่ยนแปลงไปเป็นโมโนคลินิกได้ง่าย และหลังจากการทำอิทธิพริทเมนต์ จะเกิดรอยแตกเล็กๆขึ้นบนผิวของชิ้นงาน นอกจากนี้ยังเกิดการระเหยของแมกนีเซียมและเกิดการควบแน่นกลับลงมาบนผิวของชิ้นงานใหม่ ซึ่งอาจเป็นสาเหตุทำให้สมบัติเชิงกลของ Mg-PSZ ลดลงได้.

ภาควิชาวัสดุศาสตร์

สาขาเทคโนโลยีเซรามิก

ปีการศึกษา 2547

ลายมือชื่อนิติ.....

ลายมือชื่ออาจารย์ที่ปรึกษา.....

ลายมือชื่ออาจารย์ที่ปรึกษาร่วม.....

4572374123 : MAJOR CERAMIC TECHNOLOGY

KEYWORD : Mg-PSZ/ *t-m* TRANSFORMATION / HEAT TREATMENT / HARDNESS
/STRENGTH

PAWENA THANNGAM : DEVELOPMENT OF LOW COST Mg-PSZ WITH
NANOSTRUCTURE AND HIGH MECHANICAL STRENGTH, THESIS ADVISOR : CHAIR
PROF. SHIGETAKA WADA, Ph.D., THESIS CO-ADVISOR : ASSOC. PROF. SUPATRA
JINAWATH, Ph.D., 52 pp., ISBN : 974-17-6401-4

Magnesia-Partially Stabilized Zirconia (Mg-PSZ) is an attractive ceramic material for engineering applications because it is one of the toughest sintered ceramics. It consists of a cubic zirconia matrix with a dispersion of metastable tetragonal zirconia precipitates when doped with magnesia in the range of 8-10 mol%. It is believed that the high toughness of Mg-PSZ materials is attributed to the tetragonal precipitates which nucleate and grow homogeneously within the cubic grains. Mechanical and thermal properties of Mg-PSZ are improved by controlling the microstructure through heat treatment.

The objective of this research was to study the phase transformation and mechanical properties of 8.1 mol% Mg-PSZ specimens. The samples were sintered in a temperature range from 1500 to 1700°C for 2 hours and heat treated at 1400 °C for 0.5 to 10 hours in air to avoid the prospect of eutectoid decomposition at lower temperature.

The bulk density of specimens sintered at 1700°C was 5.78 g/cm³ which was close to the theoretical density. Vickers hardness and bending strength of specimens decreased, but fracture toughness increased with increasing sintering temperature. After heat treatment, Vickers hardness and bending strength drastically decreased. The specimen sintered at lower temperature easily transformed to monoclinic phase. After annealing, many small cracks were generated on the surface. MgO evaporated and condensed on the surface of specimen. These results might be the cause of the decrement of mechanical property of Mg-PSZ.

Department Materials Science

Field of study Ceramic Technology

Academic year 2004

Student's signature.....

Advisor's signature.....

Co-advisor's signature.....

ACKNOWLEDGEMENTS

I would like to express my gratitude to my advisor, Professor Dr. Shigetaka Wada, for his encouragement, guidance and for all that I have learnt from him throughout this research. His advice inspired the good idea and motivated the research to be completed. My sincere appreciation is also expressed to my thesis co-advisor, Associate Professor Dr. Supatra Jinawath, for her kindness understanding and invaluable suggestions.

Special thanks to the staff of Department of Chemical Engineering, Faculty of Engineering, Chulalongkorn University for the kind support of phase analysis in this experiment. My thank is also extended to the staff of Scientific and Technological Research Equipment Center, Chulalongkorn University (STREC) for the help in SEM and EDS observation.

Many thanks are due to all my friends and faculty members in the Department of Materials Science for their friendship and assistance. Finally, I would like to express my deep appreciation to my family for their love, understanding and encouragement.



สถาบันวิทยบริการ
จุฬาลงกรณ์มหาวิทยาลัย

CONTENTS

	Page
Abstract (Thai)	iv
Abstract (English)	v
Acknowledgements	vi
Contents.....	vii
List of Tables.....	x
List of Figures.....	xi
Chapter 1 Introduction	1
Chapter 2 Literature review.....	3
2.1 Introduction to zirconia	3
2.2 MgO-ZrO ₂ phase system	5
2.3 Magnesia partially stabilized zirconia.....	6
2.3.1 Introduction to Mg-PSZ.....	6
2.3.2 Literature review of heat treatment of Mg-PSZ	6
2.3.3 Applications and properties of Mg-PSZ	9
Chapter 3 Experimental procedure.....	11
3.1 Raw material and characterization	11
3.1.1 Raw material	11
3.1.2 Characterization of raw material	12
3.1.2.1 Particle size distribution.....	12
3.1.2.2 Phase analysis.....	12
3.2 Sintering and characterization of the specimens	12
3.2.1 Sample preparation and experimental conditions.....	12
3.2.2 Characterization	14
3.2.2.1 Density.....	14
3.2.2.2 Microstructure.....	14
3.2.2.3 Phase analysis.....	14
3.2.2.4 Strength measurement.....	14
3.2.2.5 Vickers hardness and fracture toughness measurement...16	

CONTENTS (cont.)

	Page
Chapter 4 Results and discussions	17
4.1 Characterization of raw material	17
4.1.1 Particle size distribution.....	17
4.1.2 Phase analysis.....	18
4.2 Characterization of sintered specimens	18
4.2.1 Density.....	18
4.2.2 Phase analysis.....	20
4.2.3 Vickers hardness and fracture toughness	22
4.2.4 Bending strength.....	24
4.2.5 Microstructure of sintered specimens	24
4.3 Characterization of heat treated specimens.....	28
4.3.1 Observation of specimens.....	28
4.3.2 Phase analysis.....	28
4.3.3 Vickers hardness	29
4.3.4 Bending strength.....	31
4.3.5 Microstructures of annealed specimens	33
4.3.6 MgO content.....	34
4.4 Discussion on practical use of Mg-PSZ.....	35
Chapter 5 Conclusions	37
Chapter 6 Future work	38
References.....	39
Appendices	41
Appendix 1 Water absorption of sintered specimens	42
Appendix 2 Vickers hardness and Fracture toughness of sintered specimens.....	43
Appendix 3 XRD pattern of bottom side surface of specimen sintered at 1700°C.....	44
Appendix 4 Vickers hardness of annealed specimens	45

Appendix 5 Bending strength of specimens	48
Appendix 6 Data of MSZ 8 from ICP analysis.....	51
Biography	52



สถาบันวิทยบริการ
จุฬาลงกรณ์มหาวิทยาลัย

LIST OF TABLES

	Page
Table 2.1 Properties of Mg-PSZ with that of other two typical ceramic materials	10
Table 3.1 Characteristic properties of MSZ 8 powder	11
Table 4.1 Condition for observing the monoclinic and cubic contents.....	20



สถาบันวิทยบริการ
จุฬาลงกรณ์มหาวิทยาลัย

LIST OF FIGURES

	Page
Figure 2.1 Schematic representation of the three polymorphs of zirconia: (a) cubic, (b) tetragonal and (c) monoclinic	3
Figure 2.2 ZrO ₂ -rich portion in the phase diagram of MgO-ZrO ₂	5
Figure 2.3 TEM micrograph of tetragonal precipitates in Mg-PSZ	7
Figure 2.4 Four point bending strength (a) and Fracture toughness (K _c)(b) of Mg-PSZ as a function of ageing time at 1400°C	8
Figure 3.1 Flow chart of sample preparation and characterization	13
Figure 3.2 Flowchart of sample preparation for bending strength measurement	15
Figure 4.1 Particle size distribution of MSZ 8 powder	17
Figure 4.2 X-ray diffraction pattern of MSZ 8 powder	18
Figure 4.3 Relationship between bulk density and sintering temperature	19
Figure 4.4 Relationship between relative density and sintering temperature	19
Figure 4.5 Relationship between the ratio of monoclinic : cubic phase content and sintering temperature	20
Figure 4.6 The XRD patterns of specimens sintered at 1500°C (a) and SPA specimens (b)	21
Figure 4.7 Hardness and fracture toughness of sintered specimen as a function of sintering temperature	22
Figure 4.8 Optical micrographs of MSZ 8 sintered at 1500°C (a), 1600°C (b) and 1700°C (c)	23
Figure 4.9 Relationship between bending strength and sintering temperature	24
Figure 4.10 SEM micrograph of surface of specimen sintered at 1550°C	25
Figure 4.11 SEM micrograph of surface of specimen sintered at 1700°C	25
Figure 4.12 SEM micrographs of specimen sintered at 1500°C (a) and 1600°C (b)	26
Figure 4.13 Relationship between grain size and sintering temperature	27
Figure 4.14 Relationship between the ratio of monoclinic : cubic phase content and annealing time	28

LIST OF FIGURES (cont.)

	Page
Figure 4.15 The XRD patterns of heat treated specimens sintered at 1500°C (a) and 1700°C (b)	29
Figure 4.16 Hardness of specimens after annealing at 1400°C as a function of annealing time	30
Figure 4.17 Optical micrographs of MSZ 8 sintered at 1500°C (a), 1600°C (b) and 1700°C (c) heat treated at 1400°C for 4 h	31
Figure 4.18 Bending strength of MSZ 8 after annealing at 1400°C as a function of annealing time.....	32
Figure 4.19 SEM micrographs of fractured surfaces of specimen sintered at 1500°C (a) and specimen sintered at 1500°C, annealed at 1400°C for 4 h (b)	32
Figure 4.20 SEM micrographs of annealed specimens surfaces (a) sintered at 1500°C, ageing time 4 h, (b) sintered at 1600°C, ageing time 10 h and (c) sintered at 1700°C, ageing time 10 h.....	33
Figure 4.21 EDS pattern of specimen sintered at 1500°C and annealed at 1400°C for 4 h : (a) large grains on the background (b) background	34
Figure 4.22 MgO content of raw powder and specimen sintered at various temperatures.....	35

CHAPTER 1

INTRODUCTION

Zirconia is one of the engineering ceramics widely used, because it has noticeable properties, such as high mechanical strength, high melting point and excellent corrosion resistance. On the other hand, zirconia ceramics are restricted by the tetragonal to monoclinic phase transformation which occurs on cooling. So, zirconia can be used with its full efficiency by using a stabilizer such as MgO, CaO, CeO₂ and Y₂O₃. It can improve strength and toughness when the suitable element is added in amounts sufficient to suppress phase transformation.

Recently a new class of high performance oxide ceramics known as magnesia partially stabilized zirconia (Mg-PSZ) has been developed. Mg-PSZ consists of a dispersion of metastable tetragonal precipitates in a cubic matrix. It is one of the toughest sintered ceramics. However, its microstructure and properties may be modified by processing and heat treatment. Previous studies⁽¹⁾ have been reported that there are two heat treatments which employed to develop the microstructure. They are isothermal aging at ~1400 °C, above the eutectoid temperature and a heat treatment at 1100 °C, in the subeutectoid region. Mg-PSZ has been used for applications, e.g., lining segments for pumps, grinding balls, pistons, as well as ceramic screws for concrete constructions.

Economic reasons suggest that MgO is less expensive stabilizer than Y₂O₃. For example, prices of raw powders MgO, ZrO₂, and Y₂O₃ in market are about 150-170, 1,000-2,000 and 3,000 B/kg, respectively. Then, in this experiment we selected a commercial powder of 8.1 mol% Mg-PSZ. Some references reported that Mg-PSZ with 8.1 mol% MgO showed maximum mechanical strength when heat treated after sintering. However, the composition became cubic at above 1800 °C. No paper had disclosed the experimental results on the behavior of the composition sintered under 1700 °C.

The objective of this research was to study the phase transformation and mechanical properties of 8.1 mol% Mg-PSZ specimens sintered at lower temperature than 1700 °C and heat treated. The samples were sintered in a temperature range between 1500 to 1700°C and heat treated at 1400°C for 0.5 to 10 hours in air to avoid the prospect of eutectoid decomposition at lower temperature(2).



สถาบันวิทยบริการ
จุฬาลงกรณ์มหาวิทยาลัย

CHAPTER 2

LITERATURE REVIEW

2.1 Introduction to zirconia

Zirconia is principally derived from two sources, mainly zircon ($\text{ZrO}_2 \cdot \text{SiO}_2$) and baddeleyite (ZrO_2) which always has a small amount of hafnium oxide. Zirconia can also be prepared from many processes, for example chemical and plasma process(1,3). Zirconia has been used for many applications because of its outstanding properties, such as high toughness, wear resistance and refractoriness. Then, zirconia has been developed for applications as extrusion dies, machinery wear parts and piston caps. Ionically conducting ZrO_2 can be used as a solid electrolyte in oxygen sensors, fuel cells and furnace elements.

Pure zirconia exhibits three well defined polymorphs. The cubic structure is stable at the highest temperatures, between the melting point (2680°C) and 2370°C . The tetragonal form is stable at intermediate temperatures (2370 - 1170°C) and the monoclinic form stable at lower temperatures, as shown schematically in Fig. 2.1.

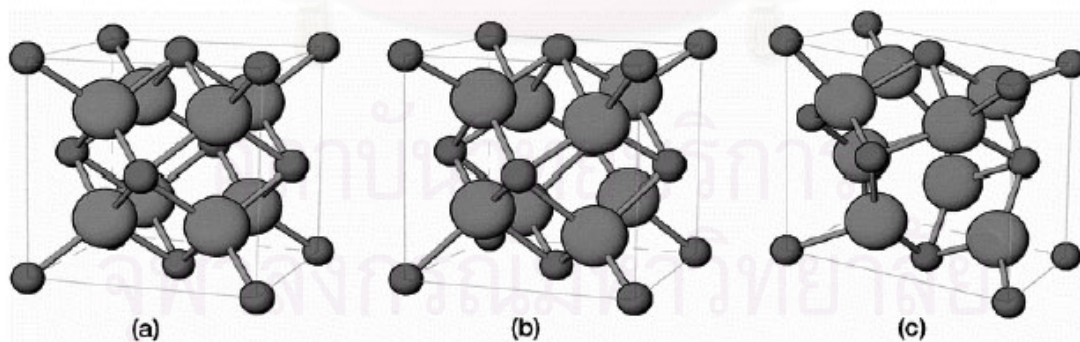


Figure 2.1 Schematic representation of the three polymorphs of zirconia: (a) cubic, (b) tetragonal and (c) monoclinic (2)

Normally, the tetragonal to monoclinic phase transformation occurs at $\sim 1000^\circ\text{C}$ on cooling(1,2,4). Thermal cycling through the transformation temperature causes

cracking, decreasing the Youngs' modulus and the strength because a volume expansion of 3-5% accompanies transformation, although it increases the resistance to catastrophic failure.

To obtain high performance zirconia materials, it is modified by controlling the amount of metal oxide additives such as MgO, CaO and Y_2O_3 because these oxides can form stable solid solutions with the cubic fluorite structure. Thus, the addition of stabilizer can be able to avoid the deleterious volume expansion which takes place at the tetragonal to monoclinic phase change.

The discovery of transformation toughened zirconia (in publishing their seminal article "Ceramic Steel") in 1972 by Garvie, Hannink and Pascoe was the first occasion to realize the potential of zirconia for increasing both the strength and toughness by utilizing the tetragonal to monoclinic phase transformation of metastable tetragonal particles induced by the presence of the stress field ahead of a crack(5,6). Then, the volume change and the shear strain developed in the martensitic reaction were recognized as opposing the opening of the crack and therefore acting to increase the resistance of the ceramic to crack propagation.

Zirconia based transformation toughening ceramics (ZTC) are presently the toughest conventionally processed oxide engineering ceramics available to industry. The two most commonly utilized zirconia based systems are partially stabilized zirconia (PSZ) and tetragonal zirconia polycrystals (TZP). TZP is a zirconia based ceramic where the matrix grains are stabilized, generally, to a single phase tetragonal form at room temperature(7).

Partially stabilized zirconia ceramics are generally produced by the controlled addition of oxide stabilizers in a concentration less than the amount of the complete stabilization, because fully stabilized zirconia ceramics have poor thermal shock resistance(8). The two most commonly used stabilizers to produce PSZ are calcia and magnesia (Ca-PSZ and Mg-PSZ, respectively), in order to form metastable tetragonal particles in the cubic matrix.

2.2 MgO-ZrO₂ phase system

Fig. 2.2. shows the ZrO₂-rich portion of the binary MgO-ZrO₂ phase diagram which was reported by Grain(9). The PSZ ceramic derived from this system is one of the most commonly used ZrO₂-based engineering materials, and it provides good example of the application of low-solubility stabilizing addition.

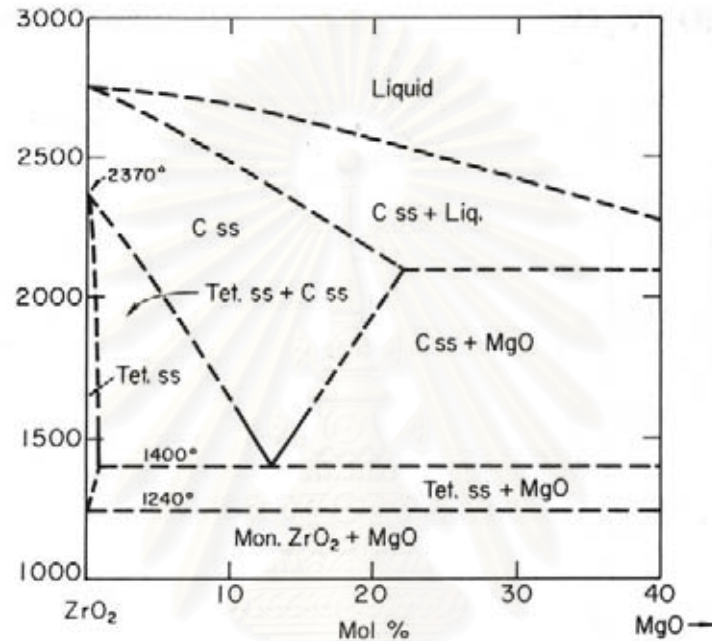


Figure 2.2 ZrO₂-rich portion in the phase diagram of MgO-ZrO₂

Commercial compositions for Mg-PSZ materials are in the range 8-10 mol% MgO. This range is preferred, because compositions with < 8 mol% MgO require too high solid-solution temperatures and the precipitation of tetragonal phase is not easily controlled. Moreover, compositions with > 10 mol% MgO do not precipitate enough volume of fractions that optimize the transformation toughening capabilities of the system. However high-purity powder should be used, especially SiO₂ is a significant contaminant, because SiO₂ preferentially reacts with the stabilizing MgO. The SiO₂ can be removed by the addition of a sintering aid which acts as scavenging oxide, such as SrO(10).

2.3 Magnesia partially stabilized zirconia

2.3.1 Introduction to Mg-PSZ

Mg-PSZ consists of a cubic matrix with a dispersion of metastable tetragonal precipitates and doped with magnesia in the range 8-10 mol%. It is one of the toughest sintered ceramics. It is reported that the maximum strength coincided with the maximum toughness in previous studies(11). It is believed that the higher toughness of Mg-PSZ materials is attributed to the tetragonal precipitates which nucleate and grow homogeneously within the cubic grains. Characteristics of Mg-PSZ indicate that mechanical and thermal properties are improved by controlling the microstructure through heat treatment. A group headed by CSIRO in Australia has been very active in this field(12). For commercial reasons, controlled cooling in sintering is more economical than heat treatment. Then Mg-PSZ materials with near maximum strength can be produced by a single firing(2).

Prolonged exposure to very high temperature can cause preferential volatilization or decomposition of certain stabilizers and thereby eventual destabilization occurs. MgO is susceptible to evaporate, however, it evaporates at the exceed 2000°C. Thus volatilization is of little importance at practical operating temperatures(11).

2.3.2 Literature review of heat treatment of Mg-PSZ

With a variety of possible heat treatments and resulting microstructure features, the Mg-PSZ systems is possibly the most complicated and interesting. The aim of the thermal treatments is, first, to develop the tetragonal precipitates to a condition of metastability so that they will transform in the presence of an applied stress or with crack propagation and, second, to maximize the volume of critical metastable tetragonal precipitates. Two ageing treatments are employed to develop the microstructure within the grain. Isothermal ageing at 1400°C allows the development of the oblate spheroids' of metastable tetragonal in cubic matrix, Fig. 2.3. The optimum properties arisen when the tetragonal precipitates have a maximum dimension of ~150-200 nm. The properties at room temperature can be further improved by a subeutectoid ageing treatment at 1100°C. The microstructure developed is complex and the subject of many investigations, notably by Hannink.

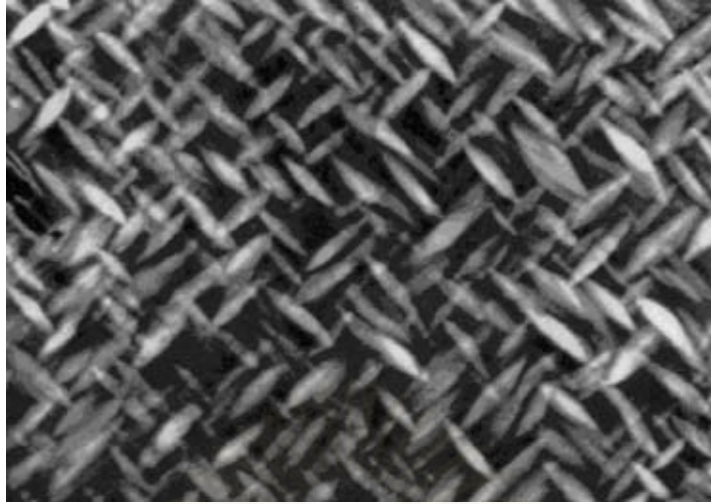


Figure 2.3 TEM micrograph of tetragonal precipitates in Mg-PSZ (13)

The sequence of precipitate coarsening in samples rapidly cooled immediately below the firing temperature typically involves a heat treatment of 1400°C . A detailed study(14) of the precipitation process in a 9.7 mol% Mg-PSZ material, using isothermal arrests imposed on a $500^{\circ}\text{C}/\text{h}$ cooling curve starting at 1700°C , has identified three precipitate forms: (i) primary, (ii) large random, and (iii) secondary.

The primary precipitates are a consequence of homogeneous nucleation and growth from a supersaturated solid solution when the material is cooled below the c -($c+t$) phase boundary. Large random precipitates occur in materials continuously cooled to room temperature from $500^{\circ}\text{C}/\text{h}$ and form preferentially at matrix inhomogeneities, such as pores and inclusions. They are more numerous in samples held isothermally at temperatures $>1400^{\circ}\text{C}$. They do not contribute to the transformation toughening behavior, because they are all monoclinic zirconia at room temperature, but may contribute to toughness through crack deflection and bridging. However, the residual internal stresses associated with their low temperature transformation can render fabricated products susceptible to accelerated chemical attack and wear. Secondary precipitate growth (SPG) occurs rapidly in the temperature range 1250 - 1400°C . SPG is nucleation controlled, with nucleus generated preferentially within c - ZrO_2 grains near grain boundaries.

Microstructure development during ageing of supersaturated solid solutions of cubic ZrO_2 stabilized with MgO was studied by Porter and Heuer in 1979(15). The starting material was a commercial 8.1 mol% Mg-PSZ . It was sintered at 1850°C for 4 hours. Optimum mechanical properties are obtained at ageing temperatures of 1400 to 1500°C , where homogeneous intragranular dispersion of small ($\sim 0.2 \mu\text{m}$ in diameter) ellipsoidal metastable tetragonal precipitates in a cubic matrix. The changes in bend strength and fracture toughness with ageing time at 1400°C are shown in Fig. 2.4. (a) and (b), respectively.

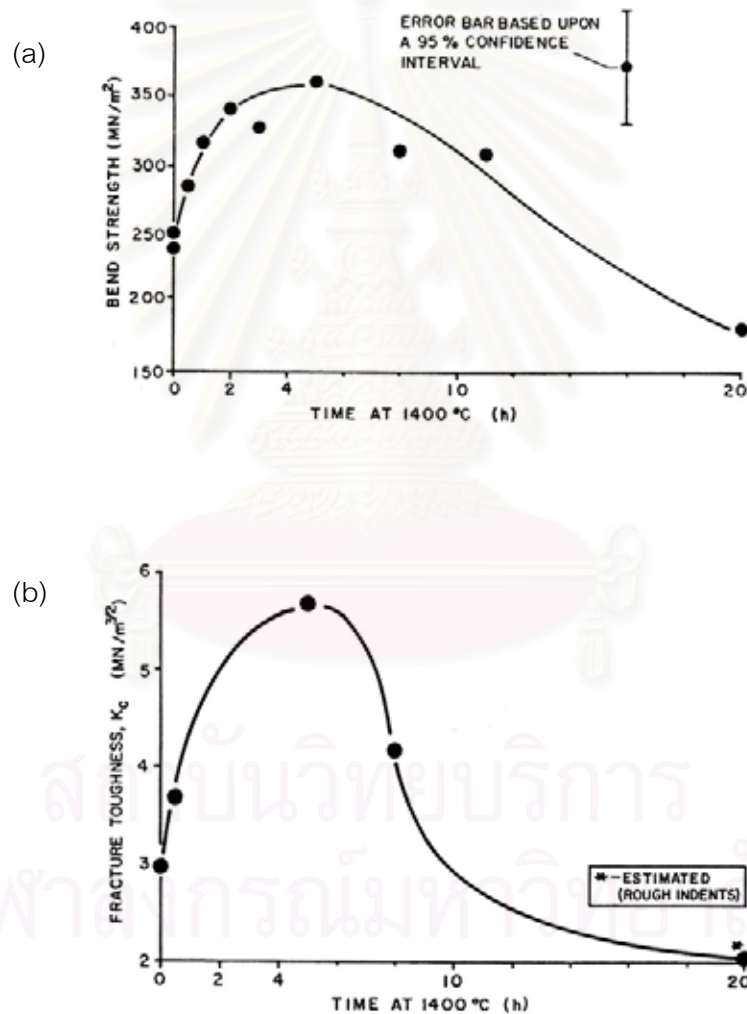
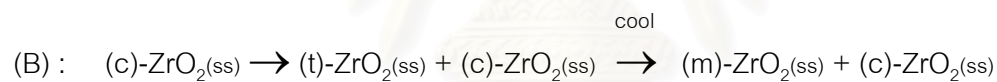
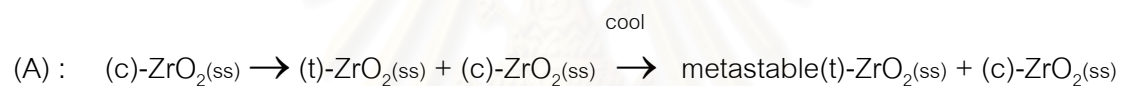


Figure 2.4 Four point bending strength (a) and Fracture toughness (K_{IC}) (b) of Mg-PSZ as a function of ageing time at 1400°C

These properties show the maximum at 4 h at 1400 °C exactly at the ageing time where the maximum volume fraction of tetragonal precipitates is produced. Thus, optimum properties are achieved with the reaction (A). Under these conditions, the particles do not transform to monoclinic symmetry when cooled to room temperature, except near propagating cracks where the stress-induced transformation contribute to the high strength and fracture toughness. Moreover, increasing ageing time leads to the further growth of the tetragonal precipitates and then they spontaneous transform to the monoclinic phase according to the reaction (B). Overageing may coincide with loss of coherency, it is certain that only small metastable tetragonal particles retain below M_s (martensitic transformation temperature). The particles are not now able to contribute to the transformation toughening mechanism and are too small to develop micro cracks. Thus, the strength and toughness of the overageing materials gradually decrease with annealing time.



It is clear that, at 1400 °C, reaction sequence (A) or (B) will be followed, depending on annealing time.

The optimally aged Mg-PSZ is under a surface residual compressive stress due to the volume expansion within a surface layer caused by tetragonal particles transform to monoclinic symmetry. This surface zone of transformation is due to evaporation of MgO during ageing(16). However, this surface zone of transformation can be avoided by “burying” samples in MgO powder during ageing

2.3.3 Applications and properties of Mg-PSZ

Due to the good mechanical, wear resistant, and thermal properties, Mg-PSZ is one of the attractive engineering materials. Mg-PSZ has been used and continues to be used for more applications, e.g., lining segments for pumps, grinding balls, pistons,

guide rollers for wire production, as well as ceramic screws for concrete constructions(3.17.18).

The properties of Mg-PSZ comparing with other materials are shown in Table 2.1 (18).

Table 2.1 Properties of Mg-PSZ with that of other two typical ceramic materials

Properties	Mg-PSZ	Y-TZP	Al ₂ O ₃
Density (g/cm ³)	5.75-5.85	6.05	3.97
Grain size (μm)	30-42	< 0.5	< 2.0
Youngs' modulus (GPa)	200	210	> 380
Bending strength (MPa)	620	1200	576
Hardness (GPa)	10.7	13	20
Fracture toughness (MPa•m ^{1/2})	10.8 ± 0.9	8	4-5
Thermal conductivity (W/mK)	2.18	2.18	29.8
Thermal expansion coefficient (x10 ⁻⁶ /°C)	10.0	10.2	8.1

สถาบันวิทยบริการ
จุฬาลงกรณ์มหาวิทยาลัย

CHAPTER 3

EXPERIMENTAL PROCEDURE

The experimental procedure including raw material characterization, techniques of sample preparation, measurements of physical and mechanical properties, and microstructure observation of sintered specimens are described in this chapter.

3.1 Raw material and characterization

3.1.1 Raw material

Starting material employed was a commercial Mg-PSZ, 8.1 mol% MgO (MSZ 8, DAIICHI KIGENSO KAGAKU KOGYO Co.,LTD, Japan). Table 3.1 shows characteristic properties of MSZ 8 given by supplier.

Table 3.1 Characteristic properties of MSZ 8 powder

Chemical analysis and properties	Quantitative data	
Chemical analysis (wt%)	SiO ₂	0.15
	Fe ₂ O ₃	0.01
	TiO ₂	0.15
	CaO	0.05
	Na ₂ O	0.05
	ZrO ₂	97.0 ± 0.2
	MgO	2.80
	H ₂ O	0.50
	lg.loss	0.50
Average particle size (µm)	0.6 ~ 0.8	
Bulk density (g/cm ³) (CIP 1 ton/cm ² : 1600°C x 2 h)	5.73	
Bending strength (MPa)	430	

3.1.2 Characterization of raw material

3.1.2.1 Particle size distribution

Particle size distribution of MSZ 8 powder was measured by a laser type particle size analyzer, CILAS 920.

3.1.2.2 Phase analysis

Crystal phase of the as-received powder was determined by an x-ray diffractometer, D8-Advanced, Bruker Co.,Ltd., operating at 40 kV, 40 mA and a count time of 1 s per 0.05° step with $\text{CuK}\alpha$ radiation. The value of 2θ was in 10° to 70° range.

3.2 Sintering and characterization of the specimens

3.2.1 Sample preparation and experimental conditions

MSZ 8 powder with 8.1 mol% MgO was well mixed with 1.0 wt% of polyvinyl alcohol (13 grams of PVA, MW 10000 – 15000, to 87 grams of water) and sieved through a 100 mesh sieve. The granules were pressed into pellets of 20 mm in diameter by a uniaxial press with 20 MPa pressure. The pressed specimens were heated to 500°C with a heating rate of $5^\circ\text{C}/\text{min}$ and held for 1 hour for binder removal, then the temperature was increased with the same heating rate to 1500, 1550, 1600, 1650 and 1700°C , dwelled for 2 hours and cooled at a rate of $5^\circ\text{C}/\text{min}$ to room temperature. After this process, the specimens were subsequently annealed at 1400°C for 0.5 to 10 hours in air. The process mentioned is schematically shown in Fig. 3.1.

สถาบันวิทยบริการ
จุฬาลงกรณ์มหาวิทยาลัย

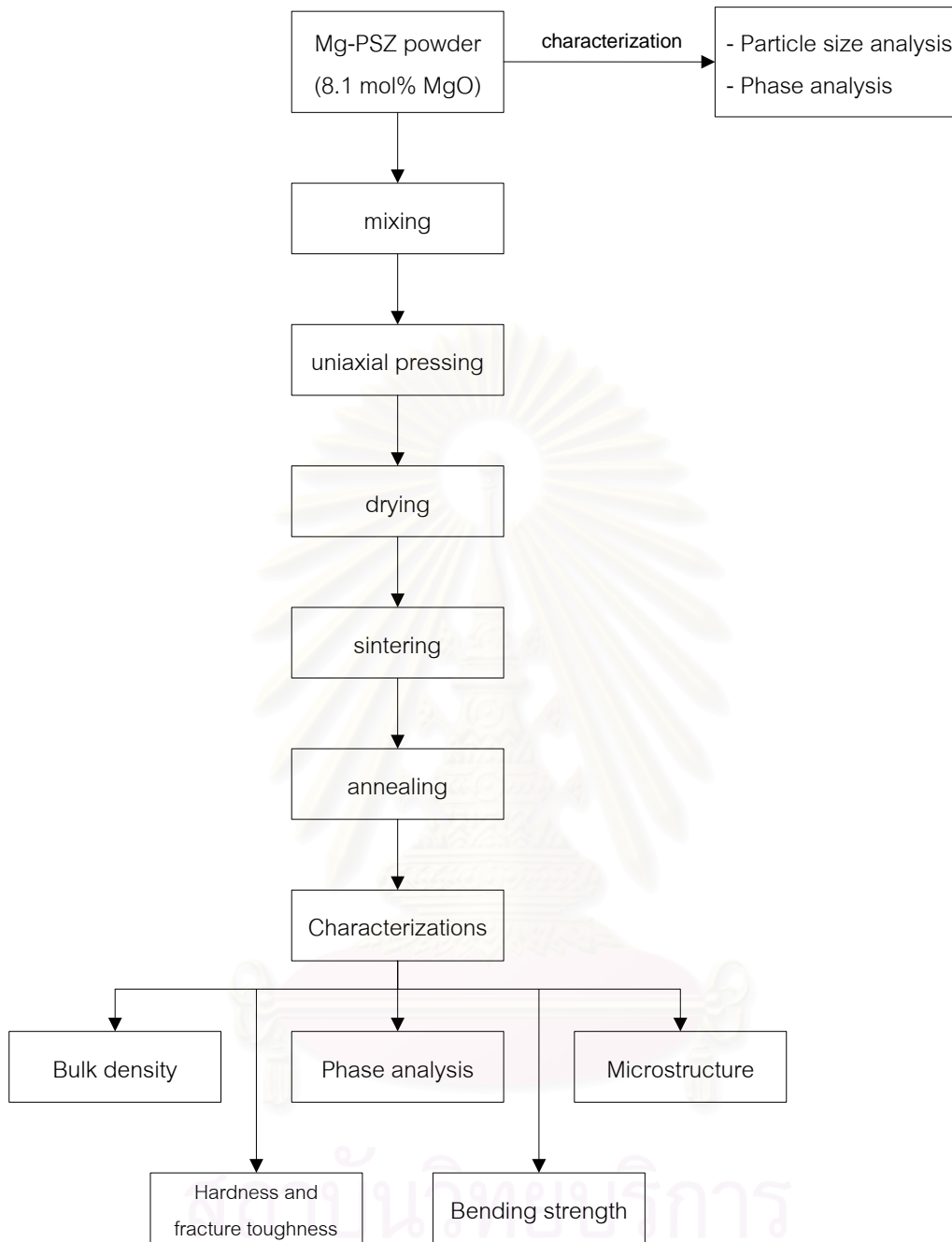


Figure 3.1 Flow chart of sample preparation and characterization

3.2.2 Characterization

3.2.2.1 Density

Both bulk density and water absorption of specimens were measured by Archimedes' method following ASTM standard (Designation : C 830-93). Then, relative density was calculated from bulk density and theoretical density. In this case, the theoretical density of 8.1 mol% Mg-PSZ is 5.79 g/cm^3 .

3.2.2.2 Microstructure

Microstructure of specimens were observed by optical microscope (OM, Olympus BX60M) and scanning electron microscope (SEM, JEOL : JSM-1670). The specimens were prepared by polishing with graded sizes of silicon carbide powder. Finally, they were polished with $1 \mu\text{m}$ diamond paste for 3 min to obtain flat and mirror-like surface. Then, polished specimens were thermally etched at 1500°C for 30 min and gold sputtered. The mean grain size was determined by line intercept method following ASTM standard (Designation : E 112-96).

3.2.2.3 Phase analysis

Crystal phases of specimen were studied by x-ray diffractometer (SIEMENS D 5000). The value of 2θ was in the range of 20° to 40° and operating at 30 kV, scanning speed of 3° per min with $\text{CuK}\alpha$ radiation.

3.2.2.4 Strength measurement

The strength of polished samples was measured in four-point bending mode according to JIS (R 1601-1981), using universal testing machine (instron). The load was applied at a crosshead speed of 0.5 mm/min at the loading points on the test specimen, and measured the maximum load at the breaking of specimen.

For this experiment, the specimens were prepared by cutting, grinding and polishing. Final dimension of test bars were of $3 \times 4 \times 40 \text{ mm}^3$. Surface of the bars were ground manually with number 2000 up to 8000 silicon carbide powder on a glass plate. Next, they were polished with $6 \mu\text{m}$ diamond paste to remove scratches and finished with $1 \mu\text{m}$ diamond paste for 3 min to get glossy surface. After polishing, specimens were cleaned up to get rid of dirt. The described sample preparation is shown in Fig. 3.2.

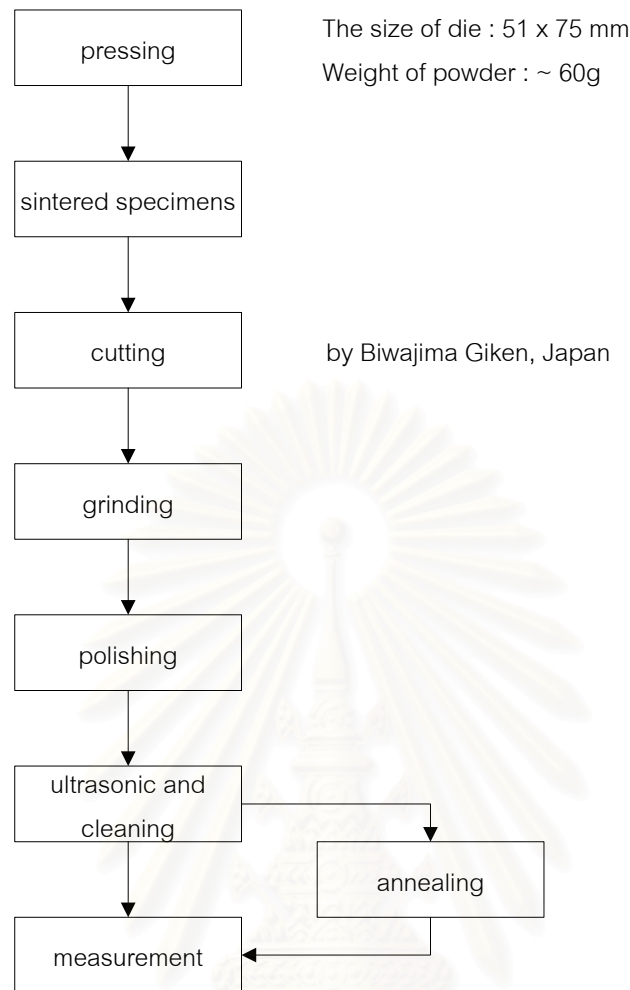


Figure 3.2 Flowchart of sample preparation for bending strength measurement

Bending strength (σ_{b4}) was calculated by the following equation :

$$\sigma_{b4} = \frac{3P(L-l)}{2wt^2}$$

σ_{b4} = 4-point bending strength, MPa

P = maximum load, N

L = distance between lower supporting points, mm

l = distance between upper loading points, mm

w = width of test specimen, mm

t = thickness of test specimen, mm

3.2.2.5 Vickers hardness and fracture toughness measurement

Vickers hardness and fracture toughness were measured by Vickers indentation method (Zwick 3212, using 15 s dwelled time at the maximum load of 10 Kg.) and calculated according to ASTM standard (Designation : C 1327-99) and JIS standard (R 1607-1995), respectively. The specimen was prepared at the same conditions which written in 3.2.2.4.

Vickers hardness (H_v) was calculated from the following equation :

$$H_v = 0.0018544 \times \left[\frac{P}{d^2} \right]$$

H_v = Vickers hardness, GPa

P = load, N

d = average length of the two diagonals of the indentation, mm

Fracture toughness (K_{Ic}) was calculated from the following equation :

$$K_{Ic} = 0.0026 \times \left[\frac{E^{1/2} P^{1/2} a}{c^{3/2}} \right]$$

K_{Ic} = fracture toughness

E = Youngs' modulus, Pa

c = crack length, m.

In this experiment, the Youngs' modulus of 8 mol% Mg-PSZ, 200 GPa (17.18), was used.

CHAPTER 4

RESULTS AND DISCUSSIONS

4.1 Characterization of raw material

4.1.1 Particle size distribution

The average particle size of MSZ 8 powder is 0.84 μm , as shown in Fig. 4.1. Thus, the particle size of raw powder measured is close to the value in the specification of supplier, 0.6-0.8 μm .

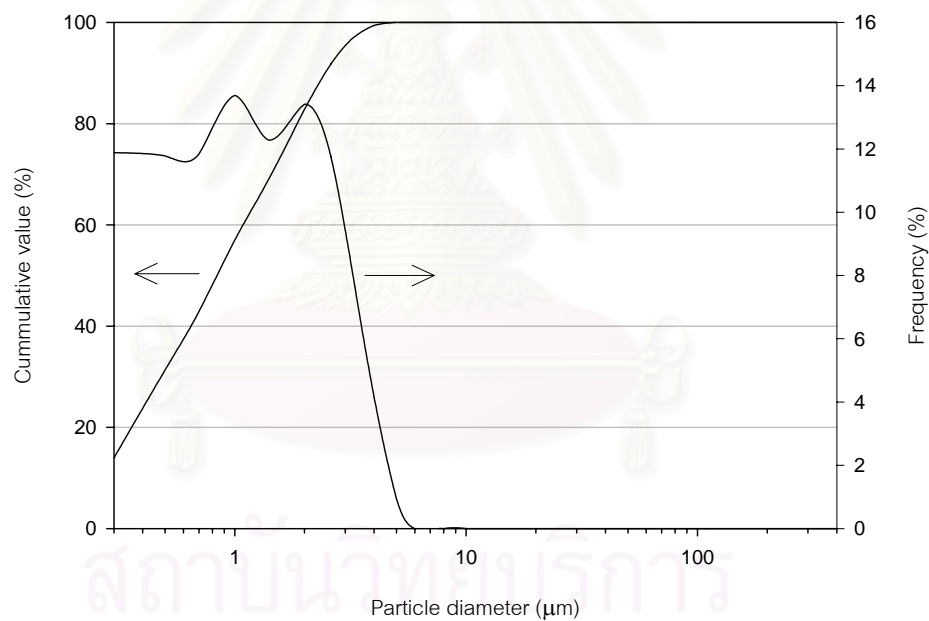


Figure 4.1 Particle size distribution of MSZ 8 powder

4.1.2 Phase analysis

The x-ray diffraction pattern of 8.1 mol% Mg-PSZ powder is shown in Fig. 4.2. The XRD pattern shows that the powder is composed of monoclinic crystal structure.

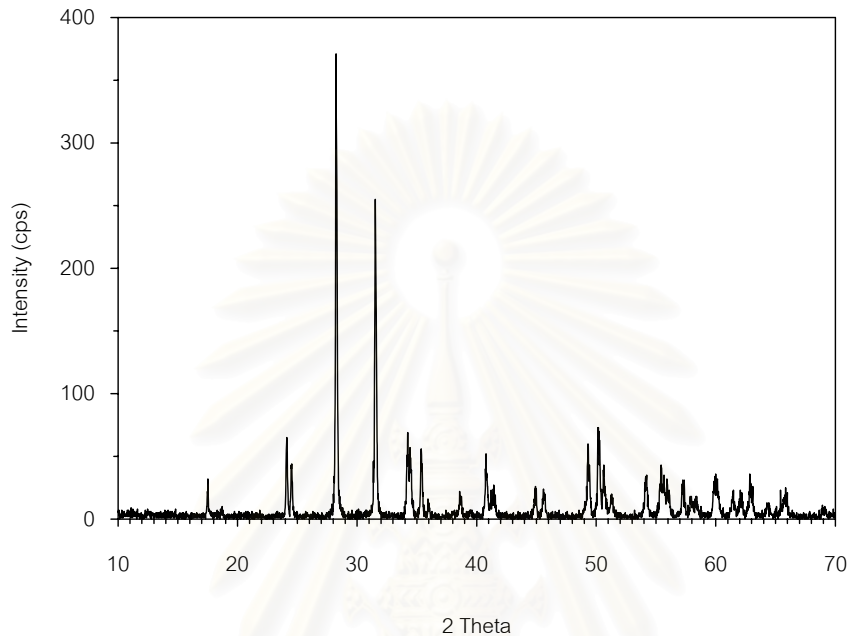


Figure 4.2 X-ray diffraction pattern of MSZ 8 powder

4.2 Characterization of sintered specimens

4.2.1 Density

The pressed specimens were sintered in a temperature range between 1350 and 1700°C, held for 2 hours. Bulk density and relative density of the specimens are shown in Fig. 4.3. and Fig. 4.4.

Bulk density of sintered specimens increased significantly with elevation of sintering temperature. The density reached almost to full density at a temperature over 1500°C. Bulk density of specimens sintered at 1650°C and 1700°C is 5.78 g/cm³ which was close to that of the theoretical density, 5.79 g/cm³. Water absorption data are attached in Appendix 1. The specimens sintered at 1500-1700°C showed very low water absorption.

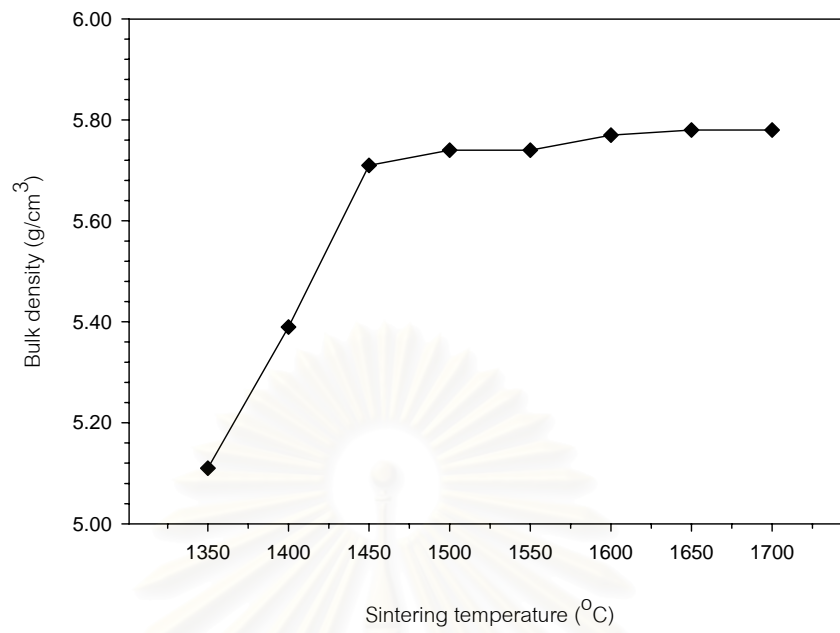


Figure 4.3 Relationship between bulk density and sintering temperature

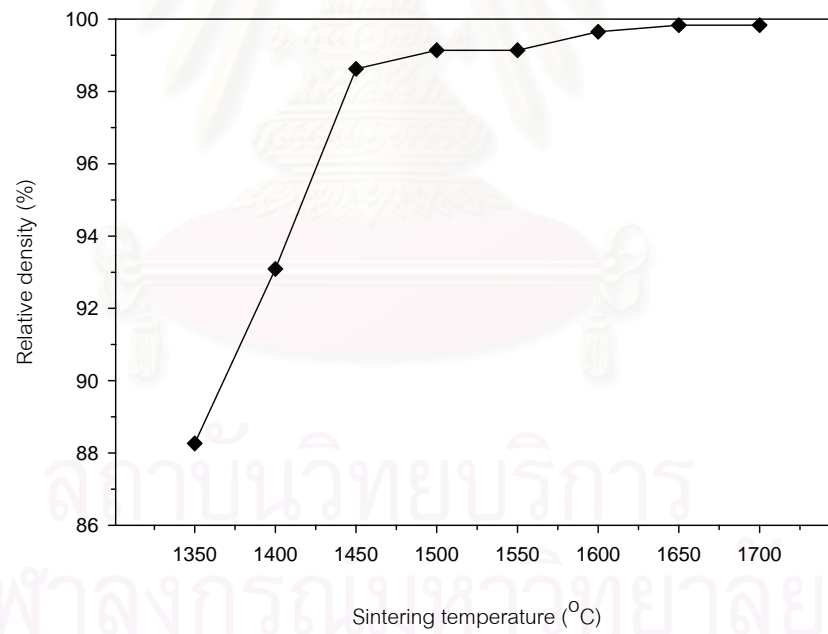


Figure 4.4 Relationship between relative density and sintering temperature

4.2.2 Phase analysis

Phase compositions of specimens were confirmed by x-ray diffractometer (XRD). The specimens were sintered at 1500, 1550, 1600, 1650 and 1700 °C. The surfaces of sintered specimens were determined in four conditions (Table 4.1) to observe the stability of tetragonal phase, because tetragonal phase in PSZ is not stable. And the stability of phase is important for the following heat treatment experiment. Monoclinic-cubic phase content of surface samples is shown in Fig. 4.5. The XRD patterns of specimens sintered at 1500 °C with conditions in Table 4.1 and SPA specimens are shown in Fig. 4.6. (a) and (b), respectively.

Table 4.1 Condition for observing the monoclinic and cubic contents

Conditions	Symbol
Sinter	Sinter
Sinter → polish	SP
Sinter → polish → anneal at 1400°C for 30 min	SPA
Sinter → anneal at 1400°C for 30 min	SA

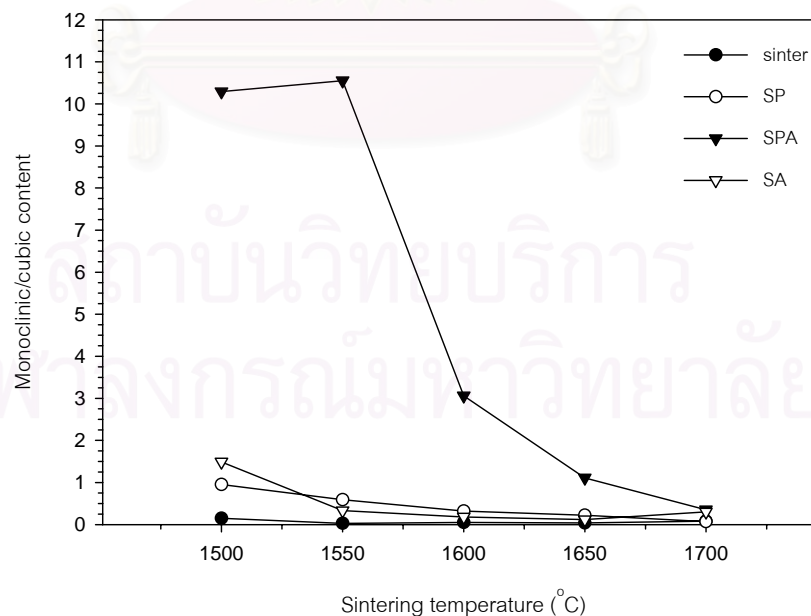


Figure 4.5 Relationship between the ratio of monoclinic : cubic phase content and sintering temperature

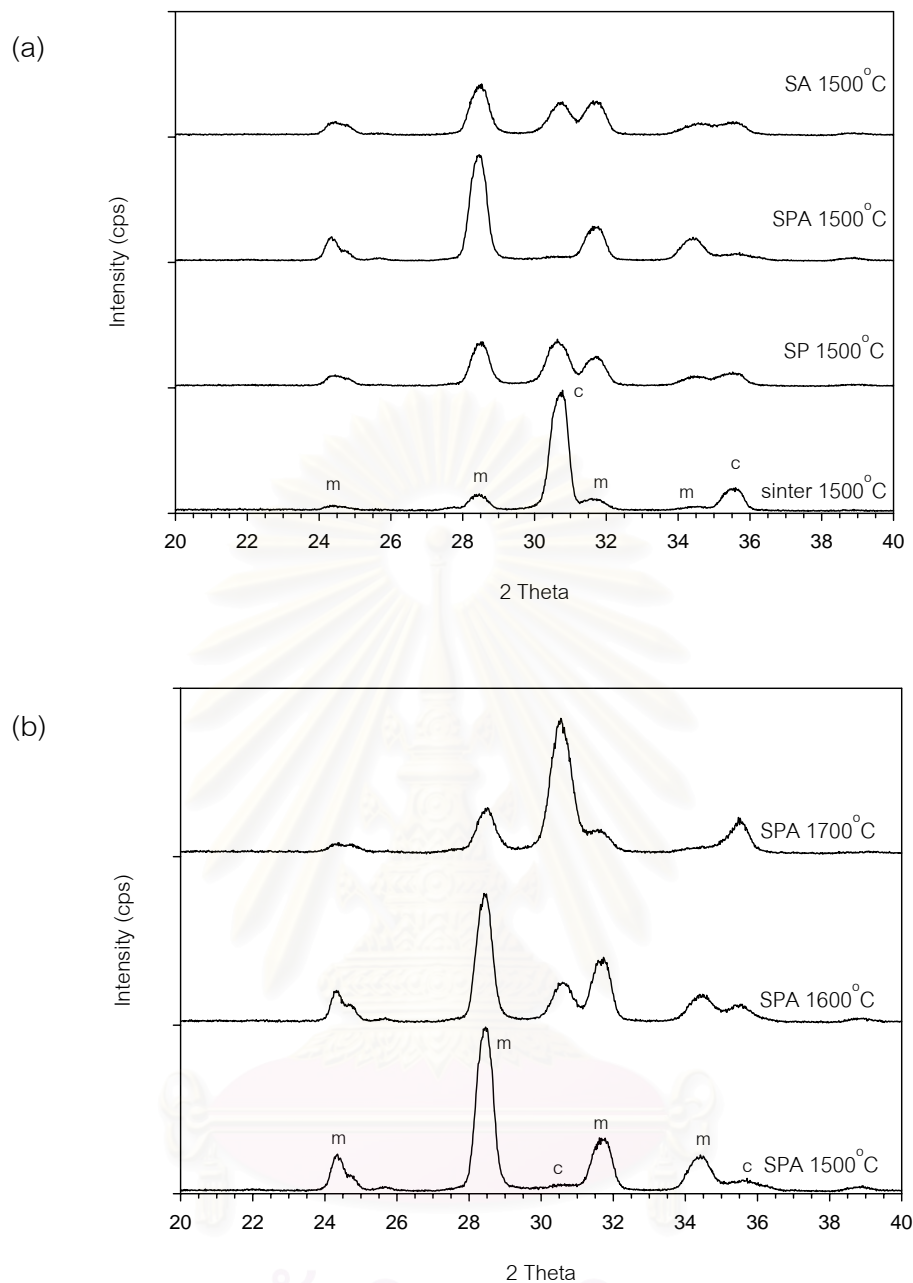


Figure 4.6 The XRD patterns of specimens sintered at 1500 °C (a) and SPA specimens (b)

X-ray analysis of bulk specimens could not be used for determining the presence or absence of $t\text{-ZrO}_2$ because of the overlap with the peaks of $c\text{-ZrO}_2$. In previous study(15), they used selected area electron diffraction (SAD) for observing. In this experiment, however we do not have this equipment. Thus we used XRD for observing crystal structure. Therefore, when we write cubic, the cubic may include tetragonal phase also. And we designated monoclinic-cubic ratio instead of tetragonal content.

Generally, as mentioned above, tetragonal phase in PSZ can transform to monoclinic by mechanical stress and annealing at high temperature. Also, the stability of tetragonal phase in Mg-PSZ is higher when it is sintered at high temperature as seen in Fig. 4.5. and Fig. 4.6. (a). In this experiment, shown in Fig. 4.5. and Fig. 4.6. (a), the extent of tetragonal to monoclinic phase transformation induced only by polishing (mechanical stress) or annealing is not so much. However, the process “ polishing → annealing ” seems to considerably accelerate the *t-m* transformation.

4.2.3 Vickers hardness and fracture toughness

Fig. 4.7. shows the Vickers hardness and fracture toughness of sintered specimens. Top view of indent of specimens sintered at 1500, 1600 and 1700°C are shown in Fig. 4.8. (a), (b) and (c), respectively. The sizes of indent and crack were measured, and the Vickers hardness and fracture toughness were calculated by the equation in 3.2.2.5. The details of all data are shown in Appendix 2.

Vickers hardness of specimen sintered at 1600°C is higher than those of the specimens sintered at 1500°C and 1700°C. The fracture toughness of sintered specimens increases significantly with increasing the sintering temperature.

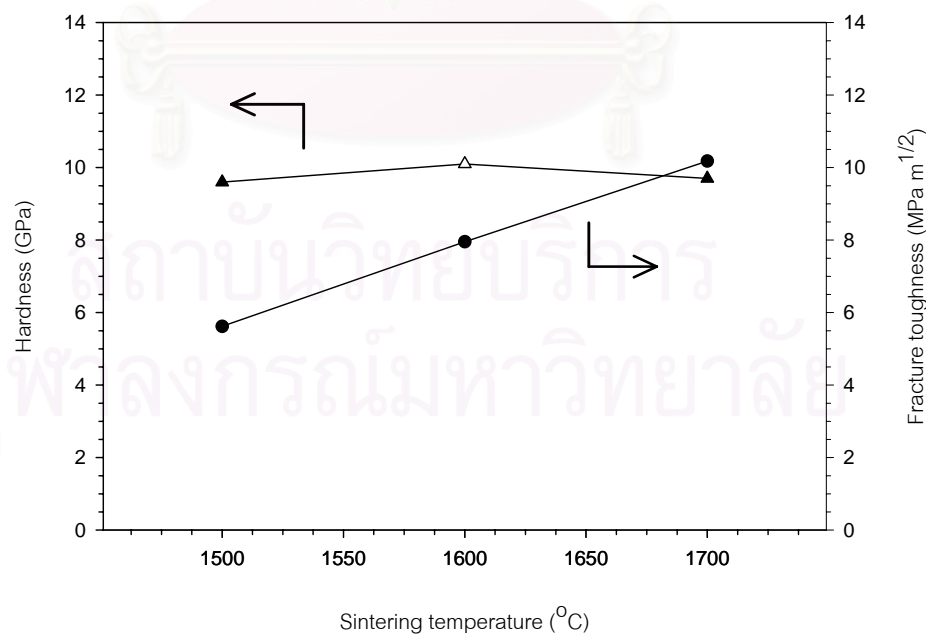


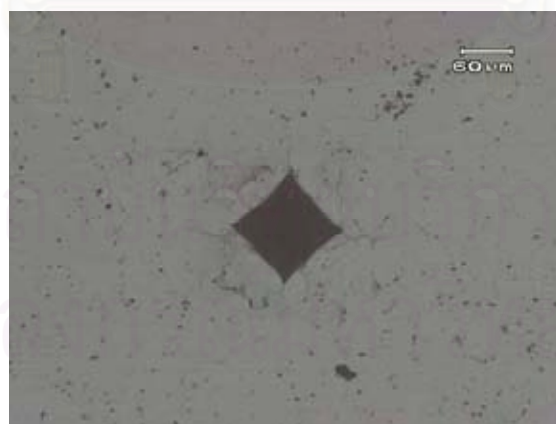
Figure 4.7 Hardness and fracture toughness of sintered specimen as a function of sintering temperature



(a)



(b)



(c)

Figure 4.8 Optical micrographs of MSZ 8 sintered at 1500°C (a), 1600°C (b) and 1700°C (c)

4.2.4 Bending strength

Bending strength of sintered specimens as a function of sintering temperature is shown in Fig. 4.9. The strength decreases with elevating sintering temperature to 1700°C. The decrement will be caused by the larger grain size shown in Fig. 4.12. and Fig. 4.13.

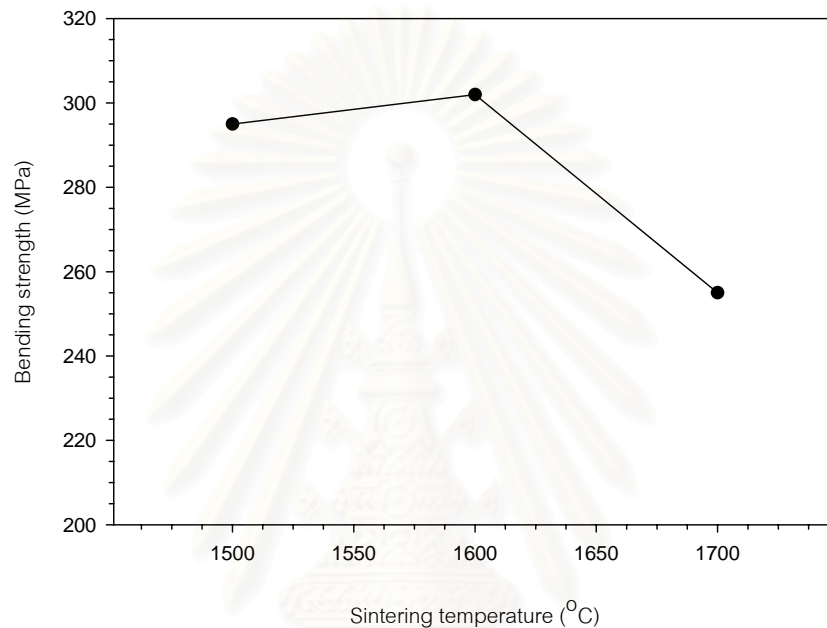


Figure 4.9 Relationship between bending strength and sintering temperature

4.2.5 Microstructure of sintered specimens

Microstructures of sintered specimens were observed by optical microscope (OM) and scanning electron microscope (SEM).

By naked eye and OM, macro-cracks were observed on the surface of sintered pellets (20 mm in diameter and 2 mm in thickness), especially at 1500°C. The number of cracks were higher on the upper surface than on the bottom surface which contacted with Al_2O_3 sagger. The number of cracks decreased with increasing sintering temperature. The cracks was not observed by OM in the specimen sintered at 1550-1700°C, but it was observed by SEM as shown in Fig. 4.10. and Fig. 4.11.

The small crack observed in the surface of pellet specimen is explained as follows : By X-ray diffractometer, top surface is almost cubic as shown in Fig. 4.5. On the

other hand, on bottom side surface, much amount of monoclinic phase was observed, the data are shown in Appendix 3 . Then, only thin surface is pure cubic and inside include some amount of tetragonal and monoclinic phases. The thermal expansion of cubic structure is higher than those of tetragonal and monoclinic structure. Therefore, it is presumed that some amount of tension stress occurred and generated cracks on the surface.

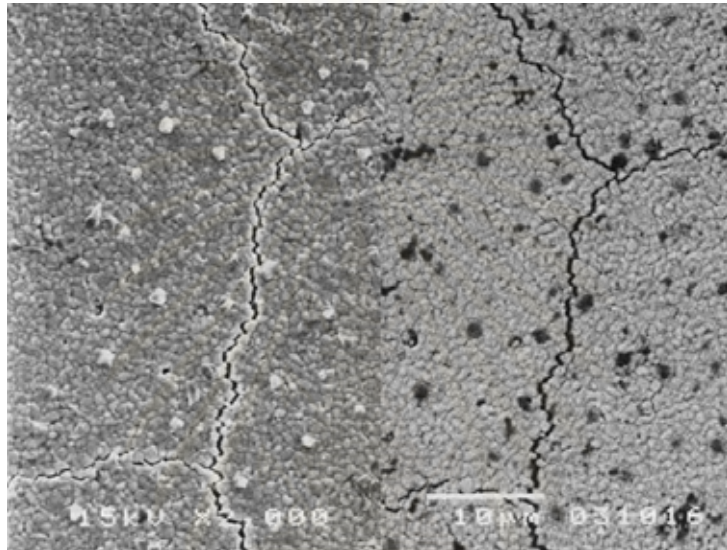


Figure 4.10 SEM micrograph of surface of specimen sintered at 1550°C

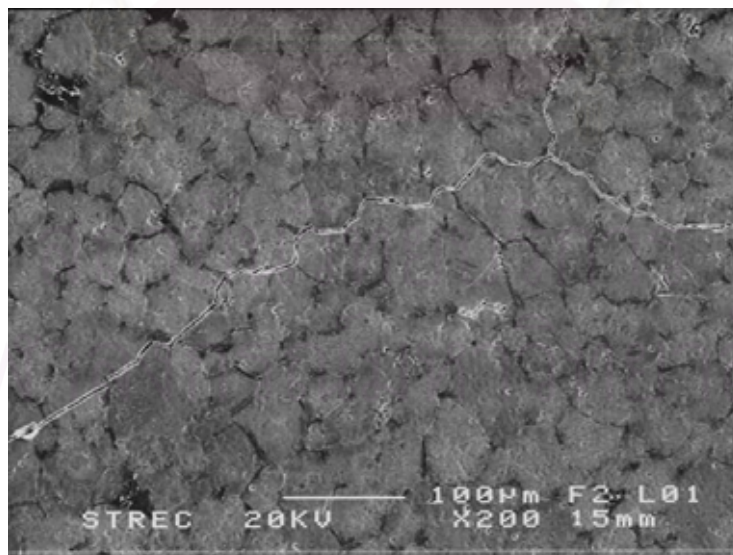
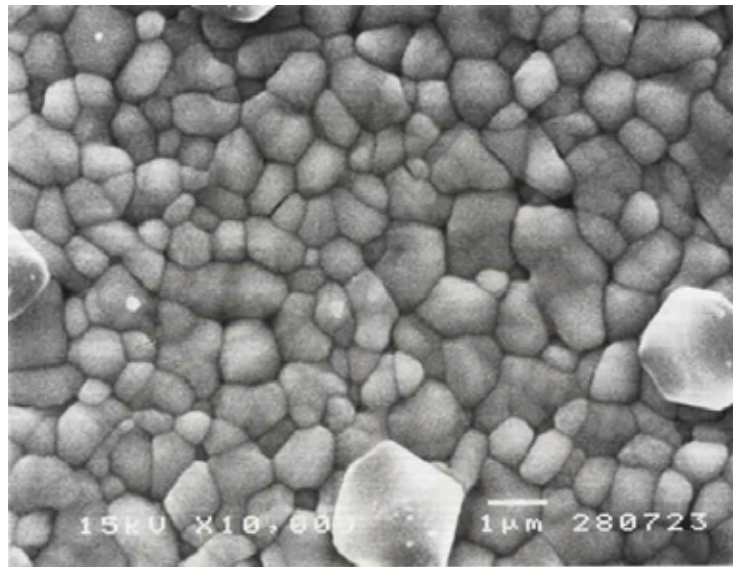
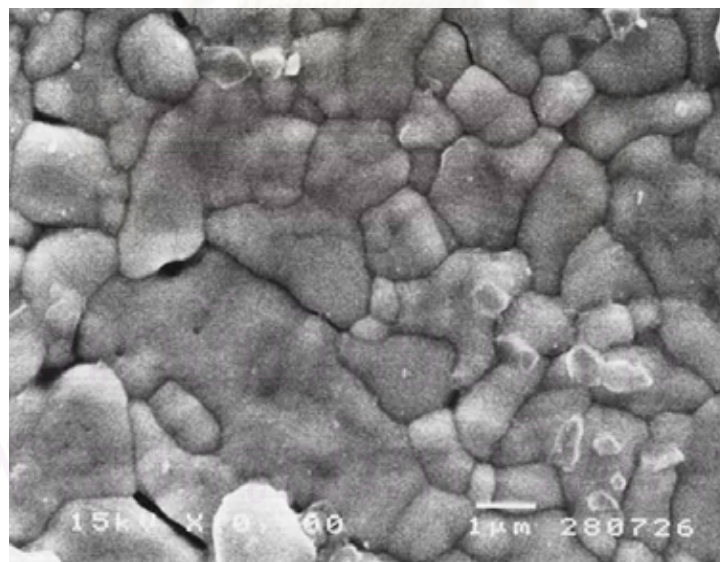


Figure 4.11 SEM micrograph of surface of specimen sintered at 1700°C

Fig. 4.12. shows the polished surface of specimens sintered at 1500°C and 1600°C and thermal etched at 1400°C, for 1 h. The micrographs reveal the development of grain growth with increasing temperature. The grain size increases with elevating sintering temperature, as shown in Fig. 4.13.



(a)



(b)

Figure 4.12 SEM micrographs of specimen sintered at 1500°C (a) and 1600°C (b)

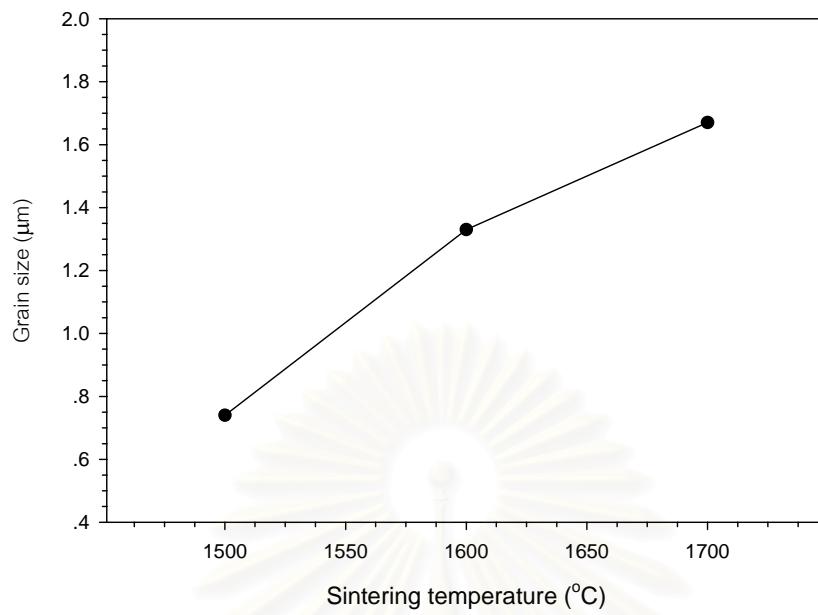


Figure 4.13 Relationship between grain size and sintering temperature

สถาบันวิทยบริการ
จุฬาลงกรณ์มหาวิทยาลัย

4.3 Characterization of heat treated specimens

4.3.1 Observation of specimens

Cracks observed in the small pellet mentioned in 4.2.5 were not observed in the plate specimen which was pressed using a die with 51 x 75 mm in width and about 6 mm in thickness. The plate specimen weights 60 g, so the heat capacity of the plate was 30 times bigger than that of the pellet. Then, it is acceptable that the surface of plate did not cool fast. As a result, there were no pure cubic phase and no crack generated.

4.3.2 Phase analysis

Phase compositions of specimens were confirmed by XRD. The specimens were sintered at 1500, 1600 and 1700°C, after this they were cut, polished and annealed at 1400°C with various annealing time. Monoclinic-cubic phase content of surface of annealed samples is shown in Fig. 4.14. The XRD patterns of heat treated specimens which sintered at 1500°C and 1700°C are shown in Fig. 4.6. (a) and (b), respectively.

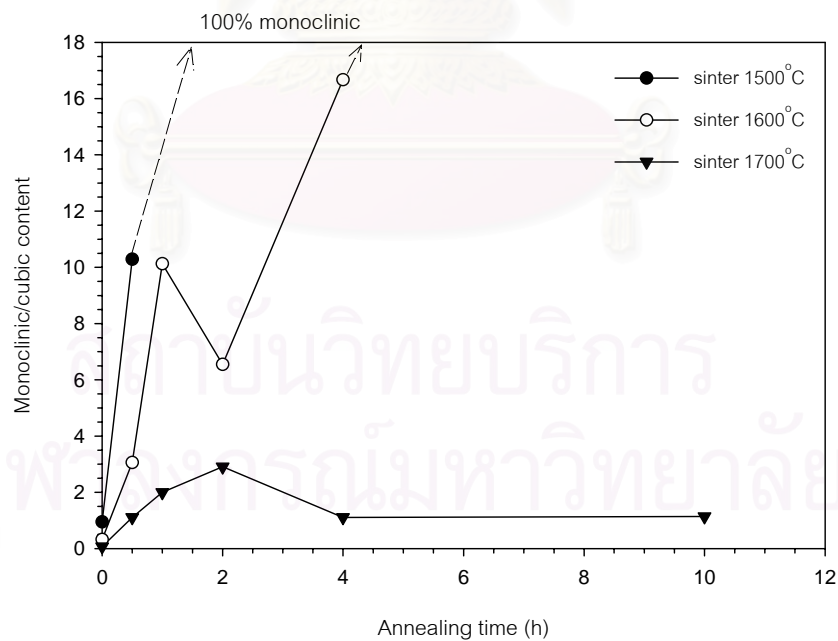


Figure 4.14 Relationship between the ratio of monoclinic : cubic phase content and annealing time

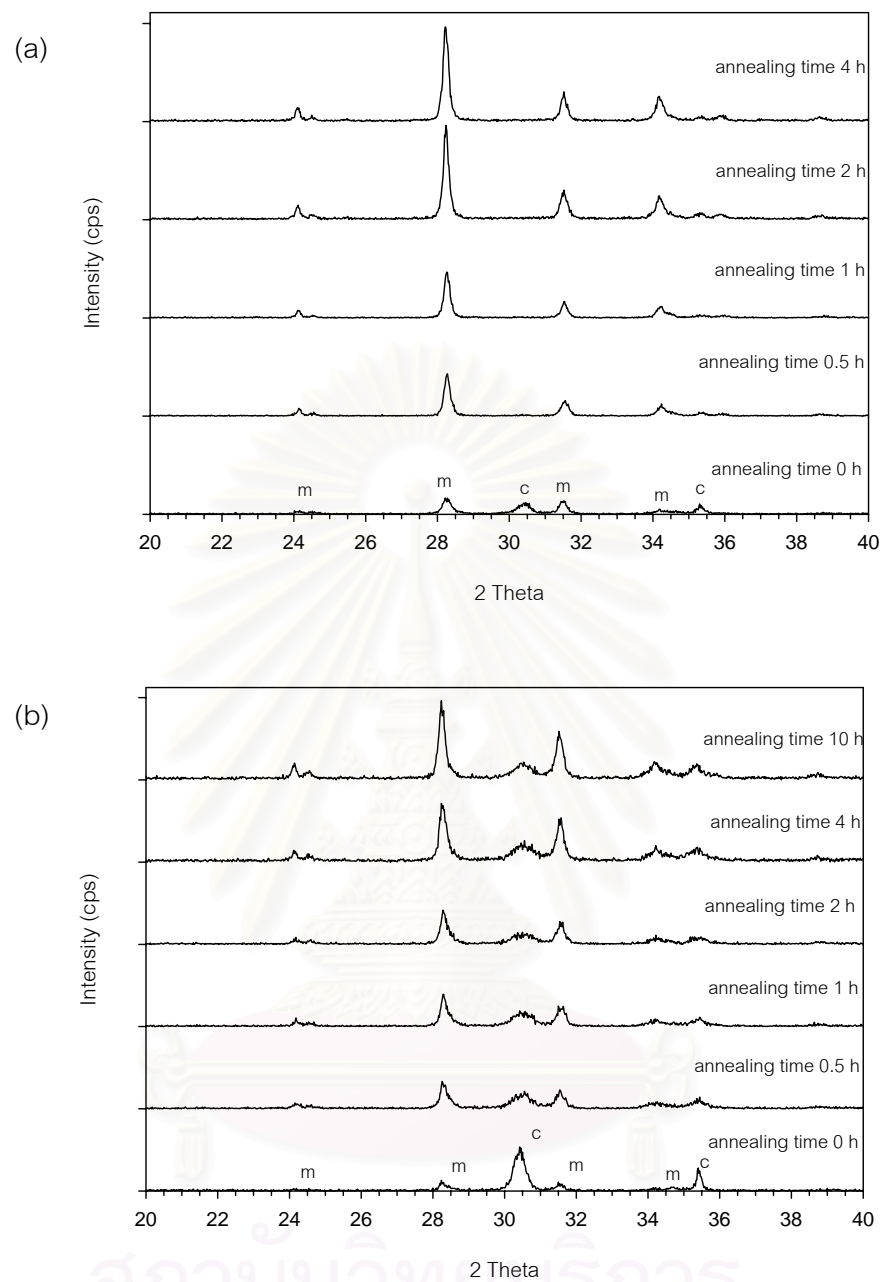


Figure 4.15 The XRD patterns of heat treated specimens sintered at 1500°C (a) and 1700°C (b)

4.3.3 Vickers hardness

Values of Vickers hardness of heat treated specimens as a function of annealing time are shown in Fig. 4.16. All details on the specimens for Vickers hardness measurement are shown in Appendix 4. The specimens were annealed at 1400°C for 0.5, 1, 2, 4 and 10 hours in air. The optical micrographs of indented specimens are shown in Fig. 4.17.

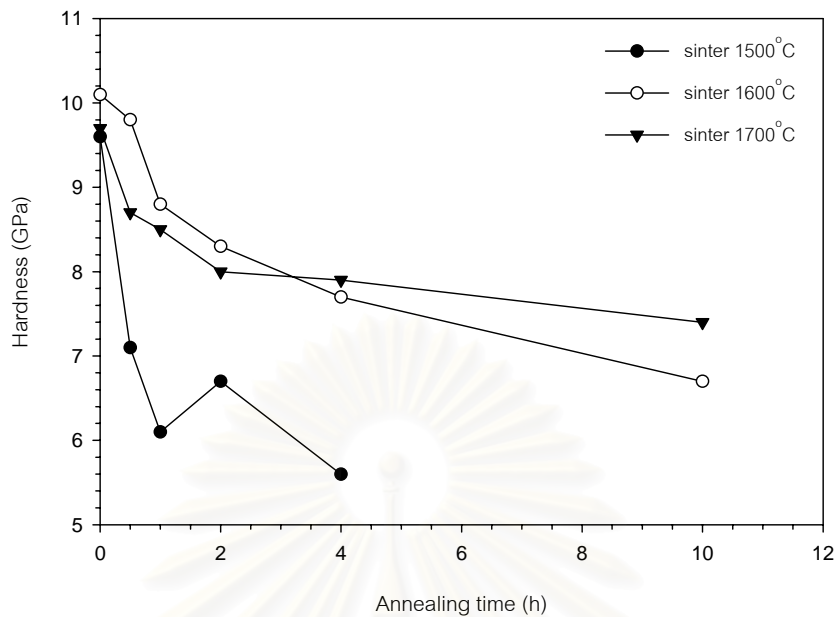


Figure 4.16 Hardness of specimens after annealing at 1400°C as a function of annealing time

From the results shown in Fig. 4.16., increasing annealing time decreases the hardness of specimens. The hardness of specimens sintered at 1600°C without annealing shows the maximum value, 10.1 MPa. The hardness of Mg-PSZ was reported as about 11.0 GPa (19) in literature. The hardnesses of specimen before annealing are 9.6~10.1 GPa. These values are close to those reported in literatures. The big decrease in hardness is not clear, but it is presumed that the decrement is related with the t - m transformation as shown in 4.3.1. Also, many small cracks are generated on the surface by annealing as shown in Fig. 4.20. These cracks might be one of the cause of the decrease in hardness.



(a)



(b)



(c)

Figure 4.17 Optical micrographs of MSZ 8 sintered at 1500°C (a), 1600°C (b) and 1700°C (c) heat treated at 1400°C for 4 h

4.3.4 Bending strength

Bending strength is presented as a function of annealing time at 1400°C in Fig. 4.18. and raw data are shown in Appendix 5. The fractured surface of specimen is shown in Fig. 4.19. The bending strength of MSZ 8 decreases with increasing annealing time. However, the decrease in strength of specimens sintered at high temperature is not so much comparing with those of specimens sintered at low temperature. The average bending strength of specimens sintered at 1600°C before annealing shows the maximum value, 302 MPa. The bending strength of Mg-PSZ was reported to be 400-600 MPa (19). Then, the strength before annealing is not so low. The degradation in strength of the annealed specimen is inversely correlated with the value of monoclinic-cubic ratio shown in Fig. 4.14. That is, increasing the value of m/c decreases the bending strength.

It is acceptable that increasing the value of m/t ratio increases the amount or size of cracks in the surface as seen in Fig. 4.20.

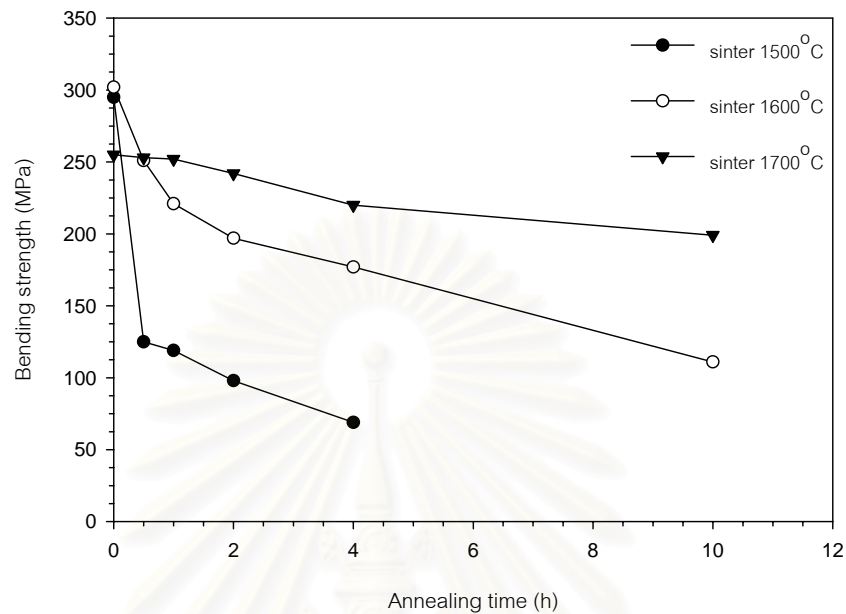


Figure 4.18 Bending strength of MSZ 8 after annealing at 1400°C as a function of annealing time

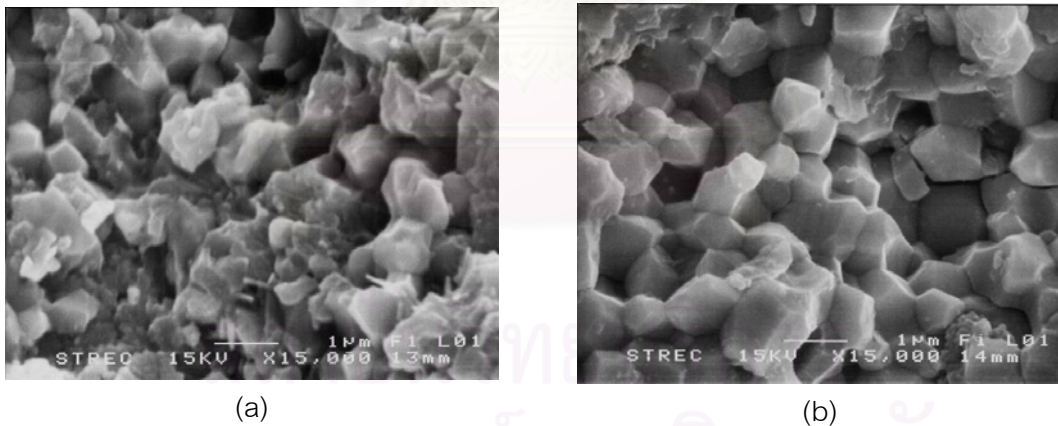


Figure 4.19 SEM micrographs of fractured surfaces of specimen sintered at 1500°C (a) and specimen sintered at 1500°C, annealed at 1400°C for 4 h (b)

Fig. 4.19. (a) shows transgranular fracture and Fig. 4.19. (b) shows intergranular fracture. This difference in fracture mode also comes from the t - m transformation, and also is one of the causes of low bending strength of annealed specimens.

4.3.5 Microstructures of annealed specimens

The surfaces of annealed specimens were observed by SEM. The specimens were annealed at 1400°C with various time. Fig. 4.20. shows the SEM micrographs of specimens sintered at 1500, 1600 and 1700°C with ageing time 4,10 and 10 h, respectively.

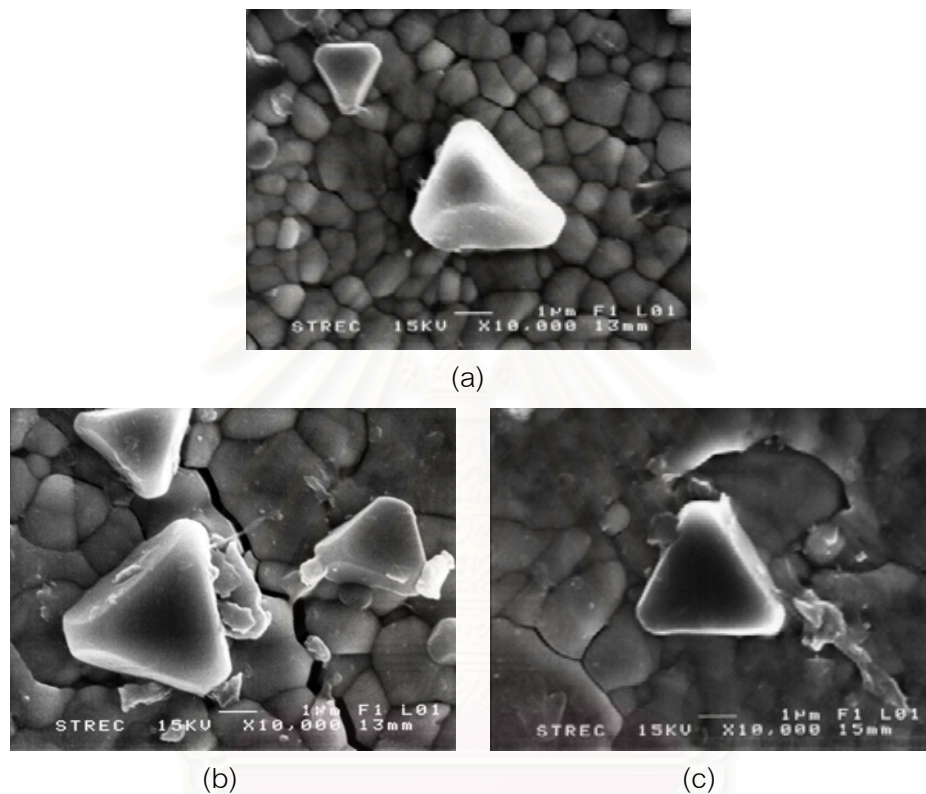
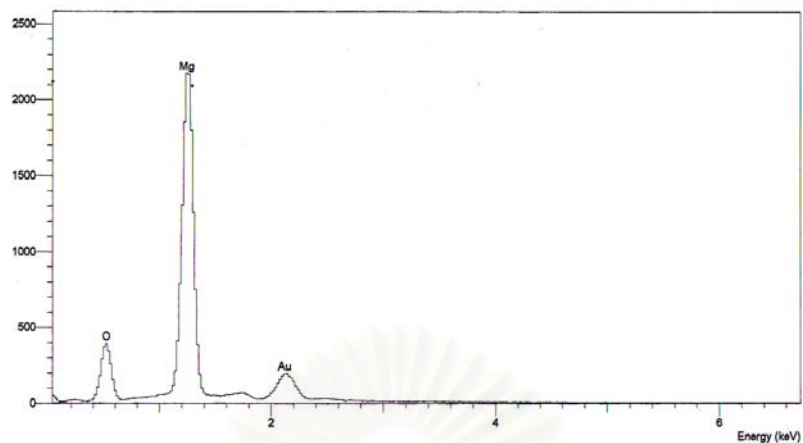
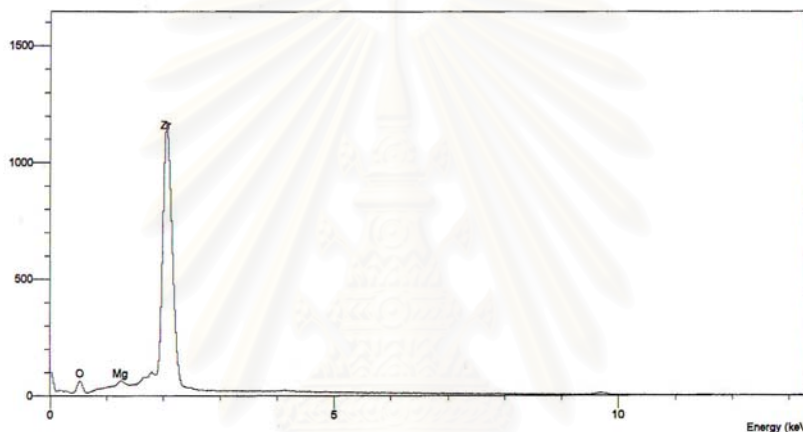


Figure 4.20 SEM micrographs of annealed specimen surfaces (a) sintered at 1500°C, ageing time 4 h, (b) sintered at 1600°C, ageing time 10 h and (c) sintered at 1700°C, ageing time 10 h

Many data on figure of crystals are observed on the surface. The number of the crystal increases with increasing annealing time. From the EDS analysis, Fig. 4.21., the large grains on the surface are MgO and the small grains are ZrO₂. Thus, from the micrographs it can be assumed that MgO evaporates during annealing process and condenses on the surface again.



(a)



(b)

Figure 4.21 EDS pattern of specimen sintered at 1500°C and annealed at 1400°C for 4 h : (a) large grains on the background (b) background

4.3.6 MgO content

SEM micrographs of annealed specimens showed the MgO evaporation during annealing process. Then, ICP analysis was used to determine the MgO content of raw powder and sintered specimens. One group of specimens was covered with MSZ 8 powder (□) and another group was covered with MgO powder (□). Relationship between MgO content and sintering temperature is shown in Fig. 4.22. The raw data of MgO content are shown in Appendix 6.

The analysis was performed three times. In the first analysis the amount of MgO in the raw powder was higher than that of sintered specimen. However, MgO content in the raw powder by the second time analysis changed from 2.5 wt% to 2.42 wt%. Also,

the result of one specimen sintered at 1700°C was 2.36 wt% by the first analysis and 2.23 wt% by the second analysis. The MgO contents in the specimen covered with MgO powder and MSZ 8 powder were expected to be more than that of specimen with no cover. However, The analyzed data are almost the same. Considering all facts mentioned above, we have to study more on how to analyze MgO in PSZ.

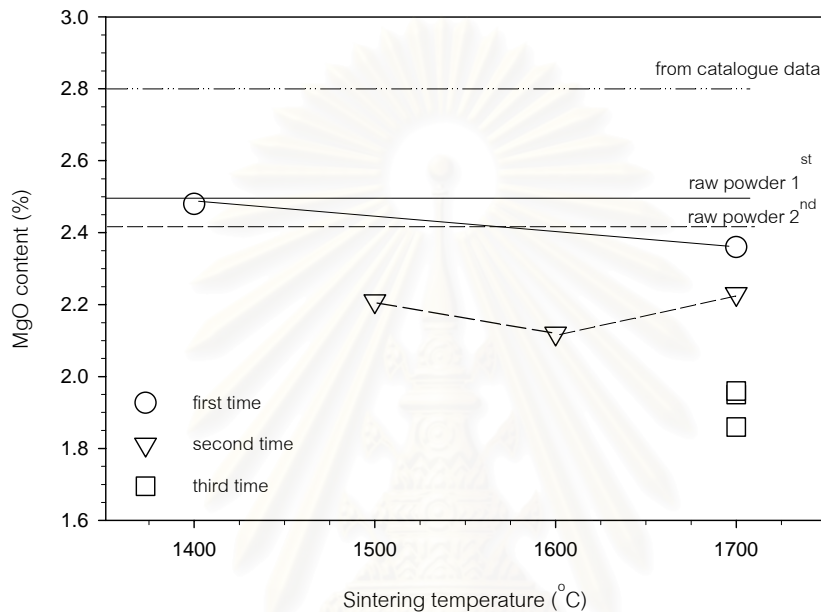


Figure 4.22 MgO content of raw powder and specimen sintered at various temperatures. (□ : covered with MSZ 8, □ covered with MgO and ■ : no cover)

4.4 Discussion on practical use of Mg-PSZ

In many literature, it had been reported that 8.1 mol% Mg-PSZ showed high strength (≥ 600 MPa) and large K_{Ic} ($10-11 \text{ MPa}\cdot\text{m}^{1/2}$) after annealing. The high mechanical strength and large fracture toughness was thought to be caused by the special morphology composed of nano-meter size tetragonal crystals ($t\text{-ZrO}_2$) precipitated in cubic crystal ($c\text{-ZrO}_2$). In the past experiments, however, pure cubic phase was realized when the composition was sintered at a temperature higher than 1800°C as understood from the phase diagram.

There have been few reports on the sintering behavior of 8.1 mol% MgO-PSZ under 1800°C. And we do not have furnace which can reach over 1700°C. However, it is also curious to know what phenomena will occur when the PSZ is sintered under the temperature of 1700°C and annealed.

The results have been reported in the previous section. Unfortunately, the result of excellent mechanical properties is not so impressive. However, many interesting information was obtained from this experiment as already reported. From all the information obtained, the potential of 8.1 mol% Mg-PSZ can be drawn as follows :

From the previous papers and the present experimental results, 8.1 mol% Mg-PSZ should be sintered at over 1800°C. Sintering a material at over 1800°C will be a shortcoming from the stand point of production cost, because at high temperature, very good refractories for furnace and also sagger are needed. When the furnace is operated at over 1800°C, refractories and sagger deteriorate in a short time and also energy consumption will be high. On the other hand, Y-TZP can be sintered to full density and it attains high mechanical strength of 600-800 MPa without annealing. Though the market price of Y_2O_3 is very expensive as 3,000 bath/kg (written in Chapter 1), the total cost of ceramics, Mg-PSZ, is not likely to be cheaper than that of Y-PSZ.

In some papers, it was reported that 9.7 mol% Mg-PSZ or 12 mol% Mg-PSZ were commercially available. Looking in the phase diagram, these compositions are pure cubic even at temperature lower than 1700°C. Several papers reported on the annealing behavior on the PSZ, however, researchers got already sintered samples from a private company and only few papers disclosed the sintering behavior of these compositions. As a result, it is likely that about 10-12 mol% Mg-PSZ will show what behavior when sintered at a temperature lower than 1700°C.

CHAPTER 5

CONCLUSIONS

1. 8.1 mol% Mg-PSZ was sintered to full density at 1600-1700°C. The cubic phase was more stable when specimen was sintered at higher temperature. However, some amount of the cubic phase transformed to monoclinic after annealing at 1400°C even the specimen was pre-sintered at 1700°C.
2. As a result of c or t→m transformation, 8.1 mol% Mg-PSZ in this experiment did not attain high mechanical strength by annealing as reported in previous papers.
3. MgO vaporized and condensed on the surface of specimen during annealing at 1400°C in air.



สถาบันวิทยบริการ
จุฬาลงกรณ์มหาวิทยาลัย

CHAPTER 6

FUTURE WORK

1. Sintering and annealing behavior of 10-12 mol% MgO-ZrO₂ should be researched in detail. Because the composition could be sintered to full density with pure cubic phase at temperature lower than 1700°C.
2. The vaporization of MgO during sintering and annealing should be made clear in detail.



สถาบันวิทยบริการ
จุฬาลงกรณ์มหาวิทยาลัย

REFERENCES

1. R. Stevens, Zirconia and Zirconia ceramics: Chemical Zirconia, second edition, Leeds: Magnesium Elektron, (n.d.).
2. R. H. J. Hannink, P. M. Kelly and B. C. Muddle, "Transformation Toughening in Zirconia-Containing Ceramics," J. Am. Ceram. Soc. 83, 3 (2000): 461-87.
3. E. William and W. M. Rainforth, Ceramic Microstructures: Property control by processing, Chapman & Hall, (1994).
4. G. K. Bansal and A. H. Heuer, "Precipitation in Partially Stabilized Zirconia," J. Am. Ceram. Soc. 58, 5-6 (1975): 235-38.
5. D. L. Porter and A. H. Heuer, "Mechanisms of Toughening in Partially Stabilized Zirconia," J. Am. Ceram. Soc. 60, 3-4 (1977): 183-84.
6. A. G. Evans and A. H. Heuer, "Review-Transformation Toughening in Ceramics: Martensitic Transformations in Crack-Tip Stress Fields," J. Am. Ceram. Soc. 63, 5-6 (1980): 241-48.
7. R. H. J. Hannink, C. J. Howard, E. H. Kisi and M. V. Swain, "Relationship between Fracture Toughness and Phase Assemblage in Mg-PSZ," J. Am. Ceram. Soc. 77, 2 (1994): 571-79.
8. T. Chraska, A. H. King and C. C. Berndt, "On the Size-Dependent Phase Transformation in Nanoparticulate Zirconia," Materials Science and Engineering. A286, (2000): 169-78.
9. C. F. Grain, "Phase Relations in the ZrO_2 -MgO System," J. Am. Ceram. Soc. 50, 6 (1994): 288-90.
10. J. Drennan and R. H. J. Hannink, "Effect of SrO Additions on the Grain-Boundary Microstructure and Mechanical Properties of Magnesia-Partially-Stabilized Zirconia," J. Am. Ceram. Soc. 69, 7 (1986): 541-46.
11. M. H. Bocanegra-Bernal and S. Diaz de la Torre, "Review Phase Transition in Zirconium Dioxide and Related Materials for High Performance Engineering Ceramics," J. Mater. Sci. 37, (2002): 4947-71.
12. S. Saito, Fine Ceramics, Ohmsha, (1987).

13. D. L. Porter and A. H. Heuer "Mechanisms of Toughening Partially Stabilized Zirconia (PSZ)," J. Am. Ceram. Soc. 60, 3-4 (1977): 183-84.
14. R. R. Hughan and R. H. J. Hannink, "Precipitation During Controlled Cooling of Magnesia-Partially-Stabilized Zirconia," J. Am. Ceram. Soc. 69, 7 (1986): 556-63.
15. D. L. Porter and A. H. Heuer, "Microstructure Development in MgO-Partially Stabilized Zirconia (Mg-PSZ)," J. Am. Ceram. Soc. 62, 5-6 (1979): 298-305.
16. T. S. Witkowski, L. Schoenlein and A. H. Heuer, "Surface Transformation in Optimally-Aged Mg-PSZ," for abstract see 4m. Ceram. Soc. Bull. 57, 9 (1978): 831.
17. F. Meschke, N. Claussen, G. de Portu and J. Rödel, "Phase Stability of Fine-Grained (Mg,Y)-PSZ," J. Am. Ceram. Soc. 78, 7 (1995): 1997-99.
18. Available from : <http://www.refractron.com>
19. Available from : <http://www accuratus.com/alumox.html>



สถาบันวิทยบริการ
จุฬาลงกรณ์มหาวิทยาลัย



APPENDICES

สถาบันวิทยบริการ
จุฬาลงกรณ์มหาวิทยาลัย

Appendix 1

Appendix 1 : Water absorption of sintered specimens

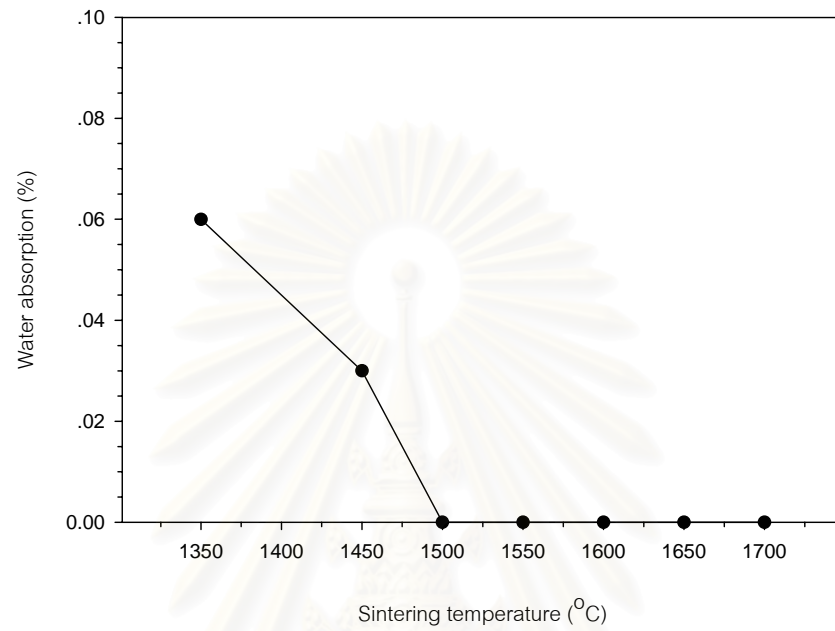


Figure I Relationship between water absorption and sintering temperature

สถาบันวิทยบริการ
จุฬาลงกรณ์มหาวิทยาลัย

Appendix 2

Appendix 2 : Vickers hardness and Fracture toughness of sintered specimens

Sintering Temperature (°C)	Micron				H _v (GPa)	K _{1c} (MPa m ^{1/2})
	Diagonal X	Diagonal Y	Crack X	Crack Y		
1500	135.66	136.98	264.25	282.36	9.8	6.1
	137.45	136.79	291.23	348.96	9.7	4.9
	138.59	137.64	396.42	326.13	9.5	4.1
	137.64	138.49	273.21	274.91	9.5	6.2
	137.45	137.64	284.91	231.79	9.6	6.7
	average				9.6	5.6
1600	134.15	133.77	237.83	246.42	10.1	7.2
	133.59	133.11	234.81	221.70	10.2	7.8
	133.77	134.81	225.00	213.96	10.1	8.4
	135.66	134.62	260.57	217.36	10.0	7.4
	132.45	134.81	220.00	211.32	10.2	8.5
	average				10.1	7.9
1700	140.00	140.76	200.00	198.83	9.2	10.1
	133.49	133.96	197.67	195.23	10.2	9.9
	135.45	138.14	196.07	192.45	9.7	10.2
	137.98	138.73	194.03	193.56	9.5	10.4
	135.95	136.02	193.15	192.45	9.8	10.3
	average				9.7	10.2

สถาบันวิทยบริการ
จุฬาลงกรณ์มหาวิทยาลัย

Appendix 3

Appendix 3 : XRD pattern of bottom side surface of specimen sintered at 1700°C

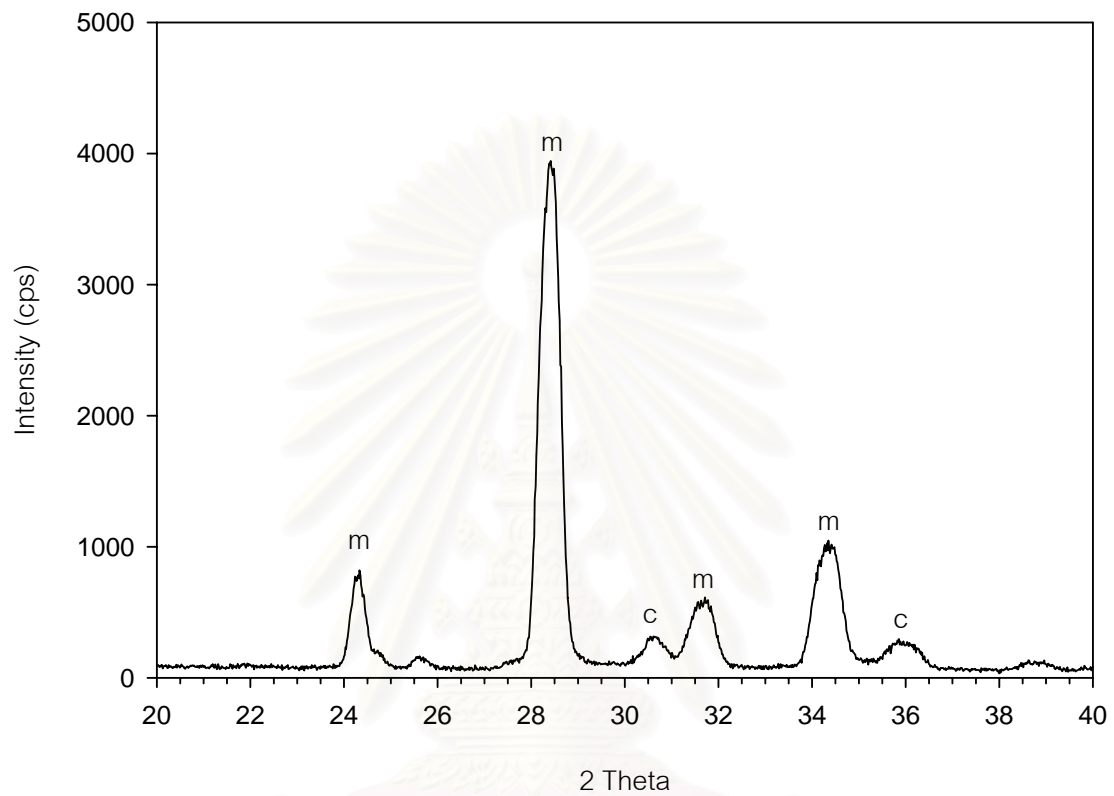


Figure II XRD pattern of bottom side surface of specimen sintered at 1700°C

สถาบันวิทยบริการ
จุฬาลงกรณ์มหาวิทยาลัย

Appendix 4

Appendix 4 : Vickers hardness of annealed specimens

Annealing time (h)	Sintering Temperature (°C)	Micron		H _V (GPa)	Average H _V (GPa)
		Diagonal X	Diagonal Y		
0	1500	135.66	136.98	9.8	9.6
		137.45	136.79	9.7	
		138.59	137.64	9.5	
		137.64	138.49	9.5	
		137.45	137.64	9.6	
	1600	134.15	133.77	10.1	10.1
		133.59	133.11	10.2	
		133.77	134.81	10.1	
		135.66	134.62	10.0	
		132.45	134.81	10.2	
	1700	140.00	140.76	9.2	9.7
		133.49	133.96	10.2	
		135.45	138.14	9.7	
		137.98	138.73	9.5	
		135.95	136.02	9.8	
0.5	1500	159.05	162.45	7.0	7.1
		158.32	157.47	7.3	
		161.89	158.19	7.1	
		158.08	159.46	7.2	
		160.43	159.95	7.1	
	1600	135.98	136.89	9.8	9.8
		135.41	136.23	9.9	
		135.02	136.41	9.9	
		136.45	135.41	9.8	
		136.07	136.87	9.8	
	1700	142.56	145.67	8.8	8.7
		143.86	146.07	8.7	
		140.20	146.83	8.8	
		142.57	145.06	8.8	
		145.86	146.31	8.5	

Annealing time (h)	Sintering Temperature (°C)	Micron		H _v (GPa)	Average H _v (GPa)
		Diagonal X	Diagonal Y		
1	1500	170.74	173.00	6.2	6.1
		173.56	172.84	6.1	
		174.86	174.63	6.0	
		173.75	172.76	6.1	
		171.82	173.43	6.1	
	1600	143.90	144.00	8.8	8.8
		143.10	143.43	8.9	
		142.57	144.13	8.9	
		143.75	143.84	8.8	
		144.23	142.90	8.8	
	1700	147.86	145.58	8.5	8.5
		146.34	147.53	8.4	
		146.27	145.34	8.6	
		145.89	146.75	8.5	
		145.11	145.95	8.6	
2	1500	164.13	162.78	6.8	6.7
		163.45	165.62	6.7	
		164.47	164.84	6.7	
		163.07	164.43	6.8	
		165.83	163.74	6.7	
	1600	148.51	147.14	8.3	8.3
		147.98	149.23	8.2	
		147.45	145.34	8.5	
		149.28	148.63	8.2	
		147.49	148.61	8.3	
	1700	149.56	148.71	8.2	8.0
		149.36	151.06	8.1	
		150.45	151.17	8.0	
		151.82	151.04	7.9	
		149.91	150.76	8.0	

Annealing time (h)	Sintering Temperature (°C)	Micron		H _v (GPa)	Average H _v (GPa)
		Diagonal X	Diagonal Y		
4	1500	181.13	180.34	5.6	5.6
		180.79	182.51	5.5	
		180.51	181.69	5.5	
		179.15	179.96	5.6	
		179.87	180.29	5.6	
	1600	151.23	153.87	7.8	7.7
		151.85	153.49	7.8	
		152.84	153.61	7.7	
		154.18	152.56	7.7	
		154.68	154.02	7.6	
	1700	150.63	151.41	8.0	7.9
		153.47	151.34	7.8	
		150.89	151.74	7.9	
		150.65	150.09	8.0	
		151.62	152.85	7.8	
10	1600	162.17	164.41	6.8	6.7
		164.59	164.96	6.7	
		164.53	164.34	6.7	
		163.64	164.72	6.7	
		162.83	163.48	6.8	
	1700	156.05	157.98	7.4	7.4
		157.34	155.87	7.4	
		158.43	156.71	7.3	
		155.62	156.47	7.5	
		156.40	157.05	7.4	

Appendix 5

Appendix 5 : Bending strength of specimens

Annealing time (h)	Sintering Temperature (°C)	Width (mm)	Thickness (mm)	Load (N)	Strength (MPa)	Average Strength (MPa)
0	1500	4.03	2.99	342	285	295
		4.02	3.00	412	341	
		4.02	3.02	316	258	
		4.03	3.00	320	265	
		4.02	3.02	345	282	
	1600	4.04	3.04	379	304	302
		4.03	3.05	368	295	
		4.03	3.06	378	301	
		4.05	3.05	384	307	
		4.05	3.05	375	299	
	1700	4.05	3.05	334	267	255
		4.05	3.05	322	257	
		4.04	3.05	311	248	
		4.05	3.04	308	247	
		4.04	3.04	315	254	
0.5	1500	4.05	3.01	147	120	125
		4.04	3.04	156	125	
		4.05	3.04	162	130	
		4.04	3.03	154	124	
		4.04	3.04	150	121	
	1600	4.04	3.01	290	226	251
		4.08	3.07	377	308	
		4.02	2.99	274	229	
		4.03	3.00	280	231	
		4.04	3.03	326	263	
	1700	4.05	3.03	277	224	253
		4.07	3.06	325	256	
		4.03	3.03	321	261	
		4.04	3.00	328	271	
		4.05	3.03	314	253	

Annealing time (h)	Sintering Temperature (°C)	Width (mm)	Thickness (mm)	Load (N)	Strength (MPa)	Average Strength (MPa)
1	1500	4.07	3.03	152	122	119
		4.04	3.04	149	120	
		4.05	3.00	132	108	
		4.07	3.05	156	124	
		4.05	3.04	150	120	
	1600	4.03	3.02	276	225	221
		4.04	3.02	271	220	
		4.04	3.02	261	213	
		4.04	3.01	269	221	
		4.03	3.01	277	227	
	1700	4.05	3.03	305	246	252
		4.05	3.03	308	249	
		4.04	3.04	319	257	
		4.04	3.04	311	250	
		4.04	3.04	320	257	
2	1500	4.07	3.04	122	97	98
		4.07	3.05	125	99	
		4.06	3.05	122	97	
		4.07	3.06	126	99	
		4.07	3.05	122	97	
	1600	4.06	3.03	279	224	197
		4.03	3.00	226	187	
		4.03	3.01	249	205	
		4.04	3.01	209	172	
		4.03	3.01	245	201	
	1700	4.08	3.04	291	232	242
		4.06	3.02	314	254	
		4.03	3.03	300	244	
		4.05	3.04	297	238	
		4.06	3.03	298	241	

Annealing time (h)	Sintering Temperature (°C)	Width (mm)	Thickness (mm)	Load (N)	Strength (MPa)	Average Strength (MPa)
4	1500	4.08	3.06	84	66	69
		4.07	3.02	92	74	
		4.06	3.05	84	67	
		4.08	3.02	85	69	
		4.07	3.03	90	72	
	1600	4.06	3.05	229	182	177
		4.06	3.06	222	175	
		4.08	3.05	216	171	
		4.04	3.00	210	173	
		4.04	3.01	224	184	
	1700	4.08	3.04	251	201	220
		4.08	3.05	283	224	
		4.07	3.05	278	220	
		4.04	3.01	279	229	
		4.07	3.02	278	225	
10	1600	4.05	3.02	134	109	111
		4.05	3.03	134	108	
		4.05	3.03	136	110	
		4.06	3.04	156	125	
		4.05	3.04	130	105	
	1700	4.06	3.02	258	209	199
		4.05	3.02	245	198	
		4.05	3.01	239	196	
		4.05	3.01	245	201	
		4.06	3.02	235	190	

Appendix 6

Appendix 6 : Data of MSZ 8 from ICP analysis

Time	Condition of specimens	MgO (%)
1	raw powder	2.5
	sintered at 1400°C	2.48
	sintered at 1700°C	2.36
2	raw powder	2.42
	sintered at 1500°C	2.21
	sintered at 1600°C	2.12
	sintered at 1700°C	2.23
3	sintered at 1700°C	1.95
	sintered at 1700°C covered with MSZ 8 powder	1.86
	sintered at 1700°C covered with MgO powder	1.96

สถาบันวิทยบริการ
จุฬาลงกรณ์มหาวิทยาลัย

BIOGRAPHY

Miss Pawena Thanngam was born on 18th of October 1979, in Chanthaburi. After graduating with a Bachelor's Degree in Materials Science from the Department of Materials Science, Faculty of Science, Chulalongkorn University in 2002, she continued a further study for Master's Degree in the field of Ceramic Technology at Chulalongkorn University and graduated in December 2004.



สถาบันวิทยบริการ
จุฬาลงกรณ์มหาวิทยาลัย